

INTENTIONALLY LEFT BLANK

CONTENTS

	Page
1. PURPOSE.....	9
2. METHOD	9
3. ASSUMPTIONS.....	10
3.1 ASSEMBLY DESIGN.....	10
3.2 HYDRAULIC FLUID COMPOSITION	10
3.3 CROSS SECTION SUBSTITUTION	10
3.4 IRON AND ALUMINUM OXIDE VOLUME EXPANSION.....	11
3.5 ASSEMBLY HARDWARE	11
4. USE OF COMPUTER SOFTWARE.....	11
4.1 MCNP	11
4.2 EXCEL.....	12
5. CALCULATION	12
5.1 INPUT PARAMETER DESCRIPTION.....	13
5.2 MATERIALS.....	13
5.2.1 Tuff Material Description	13
5.2.2 Waste Package MCNP Material Descriptions	14
5.2.3 Fuel Assembly MCNP Material Descriptions	17
5.2.4 Fuel Material.....	20
5.3 MCNP GEOMETRIC DESCRIPTIONS.....	22
5.3.1 Bounding Configuration	22
5.3.2 Fuel Assembly	23
5.4 INPUT PARAMETER SUMMARY	23
6. RESULTS	24
6.1 MAXIMUM FRESH FUEL ENRICHMENT	24
6.2 BURNED FUEL	25
6.3 WASTE STREAM COMPARISON	28
6.4 SUMMARY OF RESULTS	28
7. REFERENCES	30
8. ATTACHMENTS.....	34
ATTACHMENT I: SENSITIVITY STUDIES.....	I-1
I. DESCRIPTION AND RESULTS	I-1
I.1 ASSEMBLY LATTICE.....	I-1
I.2 FUEL DENSITY EFFECTS.....	I-3
I.3 WASTE PACKAGE FUEL ASSEMBLY GEOMETRY	I-4
I.4 OPTIMUM MODERATOR DENSITY	I-6
I.5 SIMPLIFIED GEOMETRY	I-8

CONTENTS (Continued)

	Page
I.6 TUFF EVALUATIONS.....	I-9
I.7 ABSORBER PLATE DEGRADATION	I-10
I.8 COMPROMISED FUEL RODS.....	I-11
I.9 WASTE PACKAGE INTERACTION.....	I-12
 ATTACHMENT II: ALTERNATIVE NEUTRON ABSORBER EVALUATION	 II-1
 ATTACHMENT III: ATTACHMENT CD LISTING	 III-1

FIGURES

	Page
1. Fresh Fuel k_{eff} Results	25
2. Spent Nuclear Fuel k_{eff} Results for 5.0 Wt% U-235 Initial Enrichment	27
3. Loading Curve and Projected Waste Stream.....	28
4. Fuel Assembly Lattice Design k_{eff} Results	I-3
5. Fuel Density k_{eff} Results.....	I-4
6. Standard Vertical Position Waste Package Geometry	I-5
7. Standard Horizontal Position Waste Package Geometry	I-5
8. Rotated Horizontal Position Waste Package Geometry	I-6
9. Moderator Density Sensitivity Results.....	I-7
10. Base Geometric Arrangement	II-1
11. Top View of Absorber Blocks Encased in Alloy 22	II-2
12. Side View of Absorber Blocks Encased in Alloy 22	II-2
13. Effects on k_{eff} as a function of Gd loading	II-4
14. Effects on k_{eff} as a Function of B^{10} Loading	II-4
15. Loading Curve and Waste Stream Comparison	II-5

INTENTIONALLY LEFT BLANK

TABLES

	Page
1. Tuff Material Composition.....	14
2. SB-575 N06022 Material Composition.....	15
3. Material Specifications for SA-240 S31600	16
4. Material Specifications for Ni-Gd Alloy (UNS N06464) with 1.5 wt% Gd.....	16
5. Material Specifications for Al 6061	17
6. Grade 70 A516 Carbon Steel Composition.....	17
7. Zircaloy-2 Material Composition.....	18
8. Zircaloy-4 Material Composition.....	18
9. SS304 Material Composition	19
10. Tie-Plate Component Material Volume Fractions for BWR Assembly Design	19
11. Tie-Plate Homogenized Material Compositions for BWR Fuel Assembly Design.....	20
12. Fresh Fuel Compositions.....	21
13. 7x7 BWR Fuel Assembly Specifications	23
14. Loading Curve Parameters	23
15. Fresh Fuel k_{eff} Results	24
16. Spent Nuclear Fuel k_{eff} Results	26
17. Spent Nuclear Fuel Upper Subcritical Limit Function.....	26
18. Minimum Required Burnups for Intercept of Upper Subcritical Limit	27
19. Attachment Listing.....	34
20. Tuff Composition for Sensitivity Cases	I-1
21. 8x8 and 9x9 BWR Fuel Assembly Specifications	I-2
22. 7x7 BWR Fuel Assembly Specifications	I-2
23. Fuel Assembly Lattice Design k_{eff} Results.....	I-2
24. Fuel Density k_{eff} Results.....	I-3
25. Fuel Assembly Geometry k_{eff} Results	I-6
26. Moderator Density Sensitivity Results.....	I-7
27. Simplified Geometry Results	I-8
28. External Waste Package Tuff Evaluation Results.....	I-9
29. Waste Package Tuff Internal Configuration 1 Evaluation Results.....	I-9
30. Waste Package Tuff Internal Configuration 2 Evaluation Results.....	I-10
31. k_{eff} Results for 3mm Thick Absorber Plate Cases.....	I-11
32. k_{eff} Results as a function of Absorber Plate Thickness	I-11
33. Compromised Fuel Assembly Sensitivity Cases.....	I-12
34. Waste Package Interaction Results.....	I-13
35. BWR Waste Package Configuration Neutron Absorber Sensitivity Results	II-3

INTENTIONALLY LEFT BLANK

1. PURPOSE

The objective of this calculation is to evaluate the required minimum burnup as a function of initial boiling water reactor (BWR) assembly enrichment that would permit loading of spent nuclear fuel into the 44 BWR waste package configuration as provided in Attachment IV. This calculation is an application of the methodology presented in *Disposal Criticality Analysis Methodology Topical Report* (YMP 2003). The scope of this calculation covers a range of enrichments from 0 through 5.0 weight percent (wt%) U-235, and a burnup range of 0 through 40 GWd/MTU.

This activity supports the validation of the use of burnup credit for commercial spent nuclear fuel applications. The intended use of these results will be in establishing BWR waste package configuration loading specifications.

Limitations of this evaluation are as follows:

- The results are based on burnup credit for actinides and selected fission products as proposed in YMP (2003, Table 3-1) and referred to as the *Principal Isotopes*. Any change to the isotope listing will have a direct impact on the results of this report.
- The results of 100 percent of the current BWR projected waste stream being able to be disposed of in the 44-BWR waste package with Ni-Gd Alloy absorber plates is contingent upon the referenced waste stream being sufficiently similar to the waste stream received for disposal.
- The results are based on 1.5 wt% Gd in the Ni-Gd Alloy material and having no tuff inside the waste package. If the Gd loading is reduced or a process to introduce tuff inside the waste package is defined, then this report would need to be reevaluated based on the alternative materials.

This calculation is subject to the Quality Assurance Requirements and Description (QARD) (DOE 2004) because it concerns engineered barriers that are included in the *Q-List* (BSC 2004i, Appendix A) as items important to safety and waste isolation.

2. METHOD

The method used to perform the reactivity calculations involves the simulation of the burnup and decay of fuel assemblies, for various initial enrichments and spent nuclear fuel (SNF) burnups, and the calculation of k_{eff} for the loaded waste package configuration. The isotopic compositions for SNF were calculated in Wimmer (2004) and used as input to the MCNP code (CRWMS M&O 1998b) to calculate k_{eff} for the waste package loaded with various burnup/enrichment pairs. The k_{eff} calculations are based on taking credit for burnup with a subset of the total isotopes present in commercial SNF known as the *Principal Isotopes* (YMP 2003, Table 3-1).

The k_{eff} calculations were performed using continuous-energy neutron cross-section libraries as selected in the *Selection of MCNP Cross Section Libraries* report (CRWMS M&O 1998c, pp. 61-68). The SNF from the various burnup/enrichment pairs were simulated, and the results reported from the MCNP calculations were the combined average values of k_{eff} from three estimates (collision, absorption, and track length) listed in the final generation summary in the MCNP output.

Each of the waste package configurations was represented in detail using specifications for a generic General Electric (GE) 7x7 assembly design with no burnable absorber rods, and dimensions from Larsen et.al. (1976, pp. A-1 to A-3), and waste package dimensions provided in Attachment IV from the following references: BSC 2003; BSC 2004a; BSC 2004b; BSC 2004c; BSC 2004d; BSC 2004e; and BSC 2004h.

3. ASSUMPTIONS

3.1 ASSEMBLY DESIGN

Assumption: It was assumed that the GE 7x7 assembly design is the most limiting BWR fuel assembly design for reactivity calculations.

Rationale: The basis for this assumption is that several assembly designs were evaluated in Attachment I and the results show the 7x7 design to be the most reactive.

Confirmation Status: This assumption requires no further confirmation based on the stated rationale.

Use in the Calculation: This assumption is used in Sections 5 and 6.

3.2 HYDRAULIC FLUID COMPOSITION

Assumption: It was assumed that the hydraulic fluid used as an alternative moderator material was a conventional silicone fluid (polysiloxane fluid) with a viscosity of 10cSt with a degree of polymerization of four (which is necessary for a viscosity of 10 cSt at 25°C (Gelest Inc. 2004, p.11).

Rationale: The basis for this assumption is that this material is a common hydraulic fluid (Gelest Inc. 2004, p. 7).

Confirmation Status: This assumption requires no further confirmation based on the stated rationale.

Use in the Calculation: This assumption is used in Attachment I.

3.3 CROSS SECTION SUBSTITUTION

Assumption: Since the zinc cross section libraries are unavailable, it was assumed that representing the zinc material composition in aluminum 6061 as aluminum would maintain the same neutronic characteristics.

Rationale: The rationale for this assumption is that the nuclear cross-sections for these two elements are sufficiently similar.

Confirmation Status: This assumption requires no further confirmation based on the stated rationale.

Use in the Calculation: This assumption is used in Section 5.2.2.

3.4 IRON AND ALUMINUM OXIDE VOLUME EXPANSION

Assumption: It was assumed that the volume expansion from the oxidation and hydration of the carbon steel and Al 6061 components followed the ratio of theoretical densities.

Rationale: The basis for this assumption is that the internal components can degrade over time and the amount present and volume will vary. This assumption is used in representations to capture these effects on system reactivity for various degrees of degradation with retention of various amounts of corrosion products.

Confirmation Status: This assumption requires no further confirmation since an adequate range for various amounts of degradation and volume occupied have been evaluated.

Use in the Calculation: This assumption is used in Attachment IV.

3.5 ASSEMBLY HARDWARE

Assumption: It was assumed that representing the upper and lower tie plate regions, and the channel for each assembly design with the same materials produces the same reactivity effects.

Rationale: The basis for this assumption is that the BWR assemblies are all designed to fit in the same area. Slight variances in the component volume fractions of the upper and lower tie plate regions are present as well as minor variances in the channel dimensions, but the basic hardware is the same. Variations in these components will produce negligible effects on system reactivity. As long as these components are represented, the desired effect on system reactivity is present.

Confirmation Status: This assumption requires no further confirmation based on the stated rationale.

Use in the Calculation: This assumption is used in Attachment I and IV.

4. USE OF COMPUTER SOFTWARE

4.1 MCNP

The baselined MCNP code (CRWMS M&O 1998b) was used to calculate the neutron multiplication factor for the various spent fuel compositions. The software specifications are as follows:

- Software Title: MCNP
- Version/Revision Number: Version 4B2LV
- Status/Operating System: Qualified/HP-UX B.10.20
- Software Tracking Number: 30033 V4B2LV (Computer Software Configuration Item Number)
- Computer Type: Hewlett Packard 9000 Series Workstations
- Computer Processing Unit number: 700887

The input and output files for the MCNP calculations are contained on a compact disc attachment to this calculation report (Attachment IV) as described in Sections 5 and 8, such that an independent repetition of the software use may be performed. The MCNP software used was (1) appropriate for the application of multiplication factor calculations, (2) used only within the range of validation as documented throughout Briesmeister (1997) and CRWMS M&O (1998a), and (3) obtained from Software Configuration Management in accordance with appropriate procedures.

4.2 EXCEL

- Software Title: Excel
- Version/Revision number: Microsoft® Excel 97 SR-2
- Computer Environment: Software is installed on a DELL OptiPlex GX240 personal computer, Civilian Radioactive Waste Management System (CRWMS) Management and Operating Contractor (M&O) tag number 150527, running Microsoft Windows 2000, Service Pack 4.

Microsoft Excel for Windows, Version 1997 SR-2, is used in calculations and analysis to manipulate the inputs using standard mathematical expressions and operations. It is also used to tabulate and chart results. The user-defined formulas, inputs, and results are documented in sufficient detail to allow an independent repetition of computations. Thus, Microsoft Excel is used only as a worksheet and not as a software routine. Microsoft Excel 1997 SR-2 is an exempt software product in accordance with LP-SI.11Q-BSC, Subsection 2, Software Management.

The spreadsheet files for the Excel calculations are documented in Attachment IV.

5. CALCULATION

This report evaluates the minimum required burnup of an assembly, for a specific initial enrichment, at which the calculated k_{eff} is equal to the critical limit (CL). The CL is the value of k_{eff} at which the configuration is potentially critical, and accounts for the criticality analysis methodology bias and uncertainty. In equation notation the CL is represented as shown in Equation 1.

$$CL(x) = f(x) - \Delta k_{EROA} - \Delta k_{ISO} - \Delta k_m \tag{Eq. 1}$$

where

- x = a neutronic parameter used for trending
- $f(x)$ = the lower bound tolerance limit function accounting for biases and uncertainties that cause the calculation results to deviate from the true value of k_{eff} for a critical experiment, as reflected over an appropriate set of critical experiments
- Δk_{EROA} = penalty for extending the range of applicability
- Δk_{ISO} = penalty for isotopic composition bias and uncertainty
- Δk_m = an arbitrary margin to ensure subcriticality for preclosure and turns the CL function into an upper subcritical limit (USL) function (it is not applicable for use in postclosure analyses because there is no risk associated with a subcritical event)

A more detailed discussion of the CL calculation is provided in YMP (2003, Section 3.5.3). A series of computer calculations were performed in order to develop a set of results that show k_{eff} versus burnup for different initial enrichments, and the minimum burnup required to reach the CL or USL.

A burnup credit loading curve depicts the relationship between the initial enrichment of a fuel assembly and the required minimum burnup needed to suppress the reactivity of that fuel assembly sufficiently to allow it to be safely loaded into the waste package. Any assembly whose burnup exceeds the required minimum burnup, given the initial enrichment of the fuel assembly, may be loaded into the waste package.

There are two time periods to consider for applicability of a loading curve - preclosure and postclosure. The preclosure time-period is the period before permanent closure of the repository and includes the operations involving handling, loading, and sealing of the waste packages. During the preclosure time period it is currently required that the system be designed such that the calculated k_{eff} be sufficiently below unity to show at least a five percent margin after allowance for the bias in the method of calculation, and the uncertainty in the experiments used to validate the method of calculation (Doraswamy 2004, Section 4.9.2.2). The postclosure time-period is the period after permanent closure of the repository throughout the 10,000-year regulatory period (10 CFR 63.2). During the postclosure time-period a variety of conditions may affect the waste package internal configurations. A process to identify configuration classes that have the potential for criticality is provided in YMP (2003, Section 3.6). YMP (2003) is the source for the postclosure methodology (Canori and Leitner 2003, PRD-013/T-016 and PRD-013/T-038). This report provides a limited search for potential configurations that provide the highest k_{eff} values.

5.1 INPUT PARAMETER DESCRIPTION

Sensitivity studies provided in Attachment I were used as the basis for the selection of parameters that maximize the resultant k_{eff} values.

5.2 MATERIALS

This section provides an overview of the materials that were selected for use in the MCNP inputs.

5.2.1 Tuff Material Description

Waste package configurations were represented with a tuff reflector since this is the composition of the drift material. The tuff composition used for the loading curve determinations is presented in Table 1.

Table 1. Tuff Material Composition

Compound	Wt%
SiO ₂	76.29
Al ₂ O ₃	12.55
FeO	0.14
Fe ₂ O ₃	0.97
MgO	0.13
CaO	0.5
Na ₂ O	3.52
K ₂ O	4.83
TiO ₂	0.11
P ₂ O ₅	0.05
MnO	0.07

Source: DTN:GS000308313211.001, mean values from file zz_sep_249138.txt

NOTE: Derived elemental/isotopic number densities for MCNP inputs are provided in Attachment IV, spreadsheet *Tuff composition.xls*, sheet *Latest_Tuff*

5.2.2 Waste Package MCNP Material Descriptions

The waste package representation for the MCNP calculations follows the description as that shown in Attachment IV. The outer barrier of the waste package was represented as SB-575 N06022, which is a specific type of nickel-based alloy as described in Table 2. The inner barrier was represented as SA-240 S31600, which is nuclear grade 316 stainless steel (SS) with tightened control on carbon and nitrogen content (ASM International 1987, p. 931; and ASME 2001, Section II, SA-240, Table 1) as described in Table 3. The fuel basket plates were represented as Ni-Gd Alloy (Unified Numbering System (UNS) designation is UNS N06464) with 1.5 wt% Gd as described in Table 4. The thermal shunts were represented as SB-209 A96061 T4 (aluminum 6061) as described in Table 5. The basket side and corner guides, and the basket stiffeners were represented as Grade 70 A 516 carbon steel as described in Table 6. Stiffeners were placed equidistant along the length of the basket in eight axial locations. Waste package basket material thicknesses were taken from the BWR drawings in Attachment IV.

The chromium, nickel, and iron elemental weight percents obtained from the references were expanded into their constituent natural isotopic weight percents for use in MCNP. This expansion was performed by: (1) calculating a natural weight fraction of each isotope in the elemental state, and (2) multiplying the elemental weight percent in the material of interest by the natural weight fraction of the isotope in the elemental state to obtain the weight percent of the isotope in the material of interest. This process is described mathematically in Equations 2 and 3. The atomic mass values and atom percent of natural element values for these calculations are from Parrington et al. (1996).

$$WF_i = \frac{A_i(At\%_i)}{\sum_{i=1}^I A_i(At\%_i)} \tag{Eq. 2}$$

where

WF_i = the weight fraction of isotope_i in the natural element

A_i = the atomic mass of isotope_i

$At\%_i$ = the atom percent of isotope_i in the natural element

I = the total number of isotopes in the natural element

$$Wt\%_i = WF_i(E_{wt\%}) \tag{Eq. 3}$$

where

$Wt\%_i$ = the weight percent of isotope_i in the material composition

WF_i = the weight fraction of isotope_i from Equation 2

$E_{wt\%}$ = the referenced weight percent of the element in the material composition

Table 2. SB-575 N06022 Material Composition

Element/ Isotope	ZAID ^a	Wt%	Element/ Isotope	ZAID	Wt%
C-nat	6000.50c	0.0150	Co-59	27059.50c	2.5000
Mn-55	25055.50c	0.5000	W-182 ^b	74182.55c	0.7877
Si-nat	14000.50c	0.0800	W-183 ^b	74183.55c	0.4278
Cr-50	24050.60c	0.8879	W-184 ^b	74184.55c	0.9209
Cr-52	24052.60c	17.7863	W-186 ^b	74186.55c	0.8636
Cr-53	24053.60c	2.0554	V	23000.50c	0.3500
Cr-54	24054.60c	0.5202	Fe-54	26054.60c	0.2260
Ni-58	28058.60c	36.8024	Fe-56	26056.60c	3.6759
Ni-60	28060.60c	14.6621	Fe-57	26057.60c	0.0865
Ni-61	28061.60c	0.6481	Fe-58	26058.60c	0.0116
Ni-62	28062.60c	2.0975	S-32	16032.50c	0.0200
Ni-64	28064.60c	0.5547	P-31	15031.50c	0.0200
Mo-nat	42000.50c	13.5000	Density = 8.69 g/cm ³		

Source: DTN: MO0003RIB00071.000

NOTES: ^a ZAID = MCNP material identifier

^b W-180 cross section libraries are not available so the atom percents of the remaining isotopes were used to renormalize the elemental weight and derive isotopic weight percents excluding the negligible 0.120 atom percent in nature contribution from W-180.

Table 3. Material Specifications for SA-240 S31600

Element/Isotope	ZAID ^a	Wt%	Element/Isotope	ZAID	Wt%
C-nat ^b	6000.50c	0.0200	Fe-54	26054.60c	3.7053
N-14 ^b	7014.50c	0.0800	Fe-56	26056.60c	60.2691
Si-nat	14000.50c	0.7500	Fe-57	26057.60c	1.4173
P-31	15031.50c	0.0450	Fe-58	26058.60c	0.1905
S-32	16032.50c	0.0300	Ni-58	28058.60c	8.0641
Cr-50	24050.60c	0.7103	Ni-60	28060.60c	3.2127
Cr-52	24052.60c	14.2291	Ni-61	28061.60c	0.1420
Cr-53	24053.60c	1.6443	Ni-62	28062.60c	0.4596
Cr-54	24054.60c	0.4162	Ni-64	28064.60c	0.1216
Mn-55	25055.50c	2.0000	Mo-nat	42000.50c	2.5000
Density ^c = 7.98 g/cm ³					

NOTES: ^a ZAID = MCNP material identifier

^b Carbon and nitrogen specifications are from ASM International (1987, p. 931) and remaining material compositions are from ASME (2001, Section II, SA-240, Table 1)

^c Density is for stainless steel 316 from ASTM (1999, G 1-90, p. 7, Table X1)

Table 4. Material Specifications for Ni-Gd Alloy (UNS N06464) with 1.5 wt% Gd^b

Element/Isotope	ZAID ^a	Wt%	Element/Isotope	ZAID	Wt%
C-nat	6000.50c	0.0100	Gd-152	64152.50c	0.0029
Mn-55	25055.50c	0.5000	Gd-154	64154.50c	0.0320
Si-nat	14000.50c	0.0800	Gd-155	64155.50c	0.2187
Cr-50	24050.60c	0.6602	Gd-156	64156.50c	0.3045
Cr-52	24052.60c	13.2247	Gd-157	64157.50c	0.2343
Cr-53	24053.60c	1.5283	Gd-158	64158.50c	0.3742
Cr-54	24054.60c	0.3868	Gd-160	64160.50c	0.3335
Ni-58	28058.60c	43.3679	Fe-54	26054.60c	0.0565
Ni-60	28060.60c	17.2778	Fe-56	26056.60c	0.9190
Ni-61	28061.60c	0.7637	Fe-57	26057.60c	0.0216
Ni-62	28062.60c	2.4717	Fe-58	26058.60c	0.0029
Ni-64	28064.60c	0.6537	S-32	16032.50c	0.0050
Mo-nat	42000.50c	14.5500	P-31	15031.50c	0.0050
Co-59	27059.50c	2.0000	O-16	8016.50c	0.0050
Density = 8.76 g/cm ³					

Source: ASTM B 932-04 2004, Table 1 and Section 8

NOTES: ^a ZAID = MCNP material identifier

^b 1.5wt% Gd is based on typical value of 75% credit (NRC 2000, p. 8-4) allowed for fixed neutron absorbers and a nominal Gd loading of 2.0 wt% for Ni-Gd Alloy

Table 5. Material Specifications for Al 6061

Element/Isotope	ZAID ^a	Wt%	Element/Isotope	ZAID	Wt%
Si-nat	14000.50c	0.6000	Mg-nat	12000.50c	1.0000
Fe-54	26054.60c	0.0396	Cr-50	24050.60c	0.0081
Fe-56	26056.60c	0.6433	Cr-52	24052.60c	0.1632
Fe-57	26057.60c	0.0151	Cr-53	24053.60c	0.0189
Fe-58	26058.60c	0.0020	Cr-54	24054.60c	0.0048
Cu-63	29063.60c	0.1884	Ti-nat	22000.50c	0.1500
Cu-65	29065.60c	0.0866	Al-27 ^b	13027.50c	96.9300
Mn-55	25055.50c	0.1500	Density ^c = 2.7065 g/cm ³		

Source: ASM International 1990, p. 102

NOTES: ^a ZAID = MCNP material identifier.

^b Zn cross-section data unavailable; therefore, it was substituted as Al-27 (See Assumption 3.3).

^c ASTM G 1-90 1999, p. 7, Table X1 indicates 2.7 g/cm³; ASME 2001, Section II, Table NF-2 indicates a converted value from 0.098 lb/in³ of 2.713 g/cm³; therefore the midpoint was used.

Table 6. Grade 70 A516 Carbon Steel Composition

Element/Isotope	ZAID ^a	Wt%	Element/Isotope	ZAID	Wt%
C-nat	6000.50c	0.2700	Fe-54	26054.60c	5.5558
Mn-55	25055.50c	1.0450	Fe-56	26056.60c	90.3584
P-31	15031.50c	0.0350	Fe-57	26057.60c	2.1252
S-32	16032.50c	0.0350	Fe-58	26058.60c	0.2856
Si-nat	14000.50c	0.2900	Density = 7.850 g/cm ³		

Source: ASTM A 516/A 516M-90 1991, p. 2, Table 1; density from ASME 2001, Sec II, Part A, SA-20, Section 14.1

NOTE: ^a ZAID = MCNP material identifier

5.2.3 Fuel Assembly MCNP Material Descriptions

The fuel assembly materials listed in this section refer to the upper and lower tie-plate materials, the cladding, and fuel plenum materials. In order to simplify the geometry the spacer grids were omitted from the MCNP representations. This is considered conservative with respect to criticality calculations for under-moderated lattices because there is less moderator displacement thereby increasing the moderator effectiveness where the spacer grids would normally be.

The cladding composition was Zircaloy-2 as presented in Table 7.

Table 7. Zircaloy-2 Material Composition

Element/Isotope	ZAID ^a	Wt%	Element/Isotope	ZAID	Wt%
Cr-50	24050.60c	0.0042	Ni-58	28058.60c	0.0370
Cr-52	24052.60c	0.0837	Ni-60	28060.60c	0.0147
Cr-53	24053.60c	0.0097	Ni-61	28061.60c	0.0007
Cr-54	24054.60c	0.0024	Ni-62	28062.60c	0.0021
Fe-54	26054.60c	0.0076	Ni-64	28064.60c	0.0006
Fe-56	26056.60c	0.1241	O-16	8016.50c	0.1250
Fe-57	26057.60c	0.0029	Zr-nat	40000.60c	98.1350
Fe-58	26058.60c	0.0004	Sn-nat	50000.35c	1.4500
Density ^b = 6.55 g/cm ³					

Source: ASTM B 811-97 2000, p. 2, Table 2

NOTES: ^a ZAID = MCNP material identifier.
^b From ASM International 1967, p. 1

The primary material components in the upper and lower tie-plate regions are SS304 (Table 9), Zircaloy-2 (Table 7), Zircaloy-4 as represented in Table 8, and moderator (represented as water at 1.0 g/cm³ density). Both the upper and lower tie-plate regions are represented with material compositions that represent the homogenization of all of the components in the regions. The homogenization of the base components into single homogenized material compositions is performed using Equations 4 through 6. The component material volume fractions were derived based on information from Larsen et. al. (1976) in the spreadsheet tie-plate-comp in Attachment IV and provided in Table 10. Table 11 presents the base case upper and lower tie-plate homogenized material compositions.

Table 8. Zircaloy-4 Material Composition

Element/Isotope	ZAID ^a	Wt%	Element/Isotope	ZAID	Wt%
Cr-50	24050.60c	0.0042	Fe-57	26057.60c	0.0045
Cr-52	24052.60c	0.0837	Fe-58	26058.60c	0.0006
Cr-53	24053.60c	0.0097	O-16	8016.50c	0.1250
Cr-54	24054.60c	0.0024	Zr-nat	40000.60c	98.1150
Fe-54	26054.60c	0.0119	Sn-nat	50000.35c	1.4500
Fe-56	26056.60c	0.1930	Density = 6.56 ^b g/cm ³		

Source: ASTM B 811-97 2000, p. 2, Table 2

NOTES: ^a ZAID = MCNP material identifier.
^b From ASM International 1990, p. 666, Table 6.

$$Homogenized\ Material\ Density = \sum_m^M [(\rho)_m (Volume\ Fraction\ in\ Homogenized\ Material)_m]$$

(Eq. 4)

where

m = a single component material of the homogenized material

M = the total number of component materials in the homogenized material

ρ = the mass density of the component material.

$$\left(\frac{\text{Mass Fraction of Component Material in Homogenized Material}}{\text{Material in Homogenized Material}} \right) = \left[\frac{(\rho)_m (\text{Volume Fraction in Homogenized Material})_m}{\text{Homogenized Material Density}} \right] \tag{Eq. 5}$$

$$\left(\frac{\text{Weight Percent of Component Material Constituent in Homogenized Material}}{\text{Homogenized Material}} \right) = \left(\frac{\text{Mass Fraction of Component Material in Homogenized Material}}{\text{Homogenized Material}} \right) \left(\frac{\text{Weight Percent of Component Material Constituent in Component Material}}{\text{in Component Material}} \right) \tag{Eq. 6}$$

Table 9. SS304 Material Composition

Element	Wt%	Element	Wt%
Carbon	0.080	Chromium	19.000
Nitrogen	0.100	Manganese	2.000
Silicon	0.750	Iron	68.745
Phosphorous	0.045	Nickel	9.250
Sulfur	0.030	Density = 7.94 g/cm ³	

Source: ASME (2001, Section II, SA-240, Table 1); Density from ASTM (1999, G 1-90, p. 7, Table X1)

Table 10. Tie-Plate Component Material Volume Fractions for BWR Assembly Design

Assembly Design	Stainless Steel Type 304	Zircaloy-2	Zircaloy-4	Moderator
Upper Tie-Plate	0.0528	0.0641	0.0458	0.8373
Lower Tie-Plate	0.1528	0.0344	0.0225	0.7903

Source: Derived in Attachment IV (spreadsheet *GEassembly_Vol.xls*)

Table 11. Tie-Plate Homogenized Material Compositions for BWR Fuel Assembly Design

Element/ Isotope	ZAID ^a	Upper Tie-Plate Wt%		Lower Tie-Plate Wt%	
		Flooded	Dry	Flooded	Dry
H-1	1001.50c	4.7396	--	3.7212	--
C	6000.50c	0.0170	0.0294	0.0408	0.0612
N-14	7014.50c	0.0212	0.0368	0.0511	0.0765
O-16	8016.50c	37.6623	0.0790	29.5532	0.0294
Si	14000.50c	0.1591	0.2759	0.3829	0.5737
P-31	15031.50c	0.0095	0.0166	0.0230	0.0344
S	16000.60c	0.0064	0.0110	0.0153	0.0229
Cr-50	24050.60c	0.1699	0.2947	0.4060	0.6082
Cr-52	24052.60c	3.4032	5.9038	8.1318	12.1834
Cr-53	24053.60c	0.3933	0.6823	0.9397	1.4079
Cr-54	24054.60c	0.0995	0.1727	0.2379	0.3564
Mn-55	25055.50c	0.4242	0.7358	1.0210	1.5297
Fe-54	26054.60c	0.8272	1.4350	1.9845	2.9732
Fe-56	26056.60c	13.4536	23.3393	32.2754	48.3561
Fe-57	26057.60c	0.3164	0.5489	0.7591	1.1373
Fe-58	26058.60c	0.0425	0.0738	0.1020	0.1528
Ni-58	28058.60c	1.3261	2.3006	3.1769	4.7597
Ni-60	28060.60c	0.5283	0.9165	1.2657	1.8963
Ni-61	28061.60c	0.0234	0.0405	0.0559	0.0838
Ni-62	28062.60c	0.0756	0.1311	0.1811	0.2713
Ni-64	28064.60c	0.0200	0.0347	0.0479	0.0717
Zr	40000.60c	35.7552	62.028	15.3981	23.0699
Sn	50000.35c	0.5283	0.9166	0.2275	0.3409
Density (g/cm ³)		1.9768 ^b	1.1395	2.3765 ^b	1.5862

Source: Derived in Attachment IV (spreadsheet *GEassembly_Vol.xls*)

NOTES: ^a ZAID = MCNP material identifier.

^b Values slightly differ in Attachment I sensitivity cases, but since they were kept constant in the sensitivity cases, there is no impact on the selected bounding representations

5.2.4 Fuel Material

The following information provides the details needed to duplicate the input file specifications. The uranium dioxide fresh fuel compositions for each uranium-235 enrichment used in this evaluation are specified in Table 12, and were calculated using Equation 7 (Bowman et al. 1995, p. 20) for each isotope based on the U-235 wt%.

Table 12. Fresh Fuel Compositions

Enrichment (wt% U-235)	Wt% U-234	Wt% U-235	Wt% U-236	Wt% U-238	Wt% Oxygen
1.5	0.0106	1.3222	0.0061	86.8098	11.8513
2.0	0.0144	1.7630	0.0081	86.3625	11.8519
2.5	0.0184	2.2037	0.0101	85.9152	11.8526
3.0	0.0224	2.6444	0.0122	85.4677	11.8533
3.5	0.0265	3.0851	0.0142	85.0202	11.8540
4.0	0.0306	3.5258	0.0162	84.5727	11.8547
4.5	0.0348	3.9665	0.0182	84.1251	11.8553
5.0	0.0390	4.4072	0.0203	83.6775	11.8560

$$U^{234} \text{ wt}\% = (0.007731) * (U^{235} \text{ wt}\%)^{1.0837}$$

$$U^{236} \text{ wt}\% = (0.0046) * (U^{235} \text{ wt}\%) \tag{Eq. 7}$$

$$U^{238} \text{ wt}\% = 100 - U^{234} \text{ wt}\% - U^{235} \text{ wt}\% - U^{236} \text{ wt}\%$$

The initial oxygen mass is calculated using Equations 8 through 10. In Equations 8 and 9 the atomic mass values (M) come from Audi and Wapstra (1995).

$$\frac{U \text{ Mass}}{\text{mol } UO_2} = \left(\sum_i \frac{\text{wt}\%_i}{M_i} \right)^{-1} \tag{Eq. 8}$$

where the weight percentages ($\text{wt}\%_i$) of the uranium isotopes (U^{234} , U^{236} , and U^{238}) in uranium for a given initial enrichment were calculated using Equation 7.

$$\frac{O \text{ Mass}}{\text{mol } UO_2} = (2)(M \text{ for oxygen}) \tag{Eq. 9}$$

$$O \text{ Mass in } UO_2 = \left(\frac{O \text{ Mass} / \text{mol } UO_2}{U \text{ Mass} / \text{mol } UO_2} \right) (U \text{ Mass in } UO_2) \tag{Eq. 10}$$

where

$U \text{ Mass in } UO_2$ is the fresh fuel uranium mass

The irradiated fuel material compositions were taken from Wimmer (2004, Section 6) and are listed in the corresponding inputs in atoms/b-cm.

5.3 MCNP GEOMETRIC DESCRIPTIONS

The drawing for the 44-BWR waste package configuration is contained electronically in Attachment IV. The MCNP representation of the 44-BWR waste package configuration follows the same description as that shown in Attachment IV for the initial (at time of loading) configuration.

When developing a loading curve, a configuration that results in the highest k_{eff} should be used in order to set an upper bounding limit that encompasses all other configurations. Therefore, the selection of a bounding configuration follows a linear progression based upon the results of other cases. Several potential configurations that could occur in the repository over a 10,000-year regulatory period were evaluated to determine which result in the highest k_{eff} values. The configurations are intended to investigate the effects on system reactivity as the waste package internal components degrade and the geometry changes. A series of configurations were evaluated with the descriptions and results provided in Attachment I. Based on the results, a combination of parameters was selected which will produce the most reactive representation for the generation of the loading curve.

5.3.1 Bounding Configuration

Based on an evaluation of the sensitivity results presented in Attachment I, the internal configuration class that results in the highest k_{eff} values for the BWR waste package during postclosure was selected for the bounding representation. This configuration is based on the waste package internals degrading slower than the waste form, with the waste form remaining in place and is representative of configuration class IP-1a from YMP (2003, Figure 3-2).

The geometric representation was based on an igneous event occurring causing the waste package and internals to heat up allowing cladding over-pressurization (and thus SNF oxidation) and thermal creep of the entire waste package. The magma from the igneous event causes the waste package to slump and become porous allowing moisture inside. The configuration is not considered to be able to hold a bathtub configuration of water therefore the system is considered dry with the exception of having enough moisture present to cause the SNF to hydrate.

Once the fuel cladding is breached, oxidation of the fuel material can occur and cause clad breach propagation (unzipping). The thermodynamically stable state for oxidized uranium is UO_3 (Einziger 1991, p. 88). If moisture is present in the atmosphere hydration may also occur (Einziger 1991, p. 88) and form the compound $\text{UO}_3(\text{H}_2\text{O})_2$ (Einziger 1991, Figure 1) otherwise known as the mineral schoepite (BSC 2004f, Attachment I, file *data0 files.zip*, file *data0.ymf*). Schoepite is more reactive than comparable enriched UO_2 (See Attachment I) and is therefore used to establish the minimum fresh fuel enrichment that can be loaded into the waste package to meet postclosure objectives. The derivation of this set of cases was made in Attachment IV (spreadsheet *schoepite.xls*, sheet *Fresh*). In order to make a proper comparison, the fresh fuel uranium mass was used as the basis for the amount of fresh schoepite that could form. Based on this the equivalent schoepite density over the active fuel region within the channel would be greater than theoretical (4.874 g/cm^3 [BSC 2004f, Attachment I, file *data0 files.zip*, file *data0.ymf*]). Therefore, it was represented at theoretical density with the active fuel length adjusted to what is necessary to conserve uranium mass.

5.3.2 Fuel Assembly

The physical dimensions for the fuel assembly design represented in the MCNP inputs are presented in Table 13.

Table 13. 7x7 BWR Fuel Assembly Specifications

Assembly Component	Specification ^b
Lattice	7x7
Fuel Pellet Outer Diameter ^a	1.23952 cm (0.488 in.)
Fuel Rod Cladding Thickness	0.08128 cm (0.032 in.)
Fuel Rod Cladding Inner Diameter	1.26746 cm
Fuel Rod Cladding Outer Diameter	1.43002 cm (0.563 in.)
Active Fuel Length	365.76 cm (144 in.)
Clad Material	Zircaloy-2
Channel Material	Zircaloy-2
Pin Pitch	1.87452 cm (0.738 in.)
Channel Inner Width ^c	13.246 cm
Channel Thickness ^c	0.3048 cm

Source: Larsen et. al. 1976, pp. A-1 to A-3

NOTES: ^a The representations use a smeared pellet density over the inner clad diameter.

^b Values in parentheses are from the source reference.

^c Channel dimensions were taken from Punatar 2001, Table 2-1.

5.4 INPUT PARAMETER SUMMARY

Based on the sensitivity studies presented in Attachment I, the following parameters listed in Table 14 were selected for use in the loading curve generation:

Table 14. Loading Curve Parameters

Parameter	Value	Selection Basis	Applicability
Fuel Material	UO ₂	Fresh fuel is more reactive than burned fuel	Preclosure
	UO ₃ (H ₂ O) ₂	Attachment I, Section I.8	Postclosure
Absorber	1.5 wt% Gd	Based on typical value of 75% credit (NRC 2000, p. 8-4) allowed for fixed neutron absorbers and a nominal Gd loading of 2.0 wt% for Ni-Gd Alloy	Preclosure and Postclosure
Moderator	Water at density of 1.0 g/cm ³	Attachment I, Section I.4	Preclosure
	Void	Less moderation between cavities of schoepite make the Ni-Gd alloy less effective as a neutron absorber due to decreased thermalization	Postclosure
Fuel Density	10.741 g/cm ³ [a]	Attachment I, Section I.2	Preclosure
	4.874 g/cm ³	Section 5.3.1	Postclosure
Reflector	100% Saturated Tuff	Attachment I, Section I.6	Preclosure
	100% Saturated Tuff	Attachment I, Section I.6	Postclosure

Table 14. Loading Curve Parameters

Parameter	Value	Selection Basis	Applicability
Geometry	Lattice array in Standard Vertical configuration (See Attachment I, Figure 6)	Attachment I, Section I.3	Preclosure
	Homogeneous fuel mixture separated by steel, aluminum, and Ni-Gd alloy plates	Attachment I, Section I.8	Postclosure

NOTE: ^a Calculated based on 98% theoretical density value of 10.96 g/cm³ for UO₂ (Todreas and Kazimi 1990, p. 296)

6. RESULTS

The loading curves for the 44 BWR waste package are presented in this section. The k_{eff} results represent the average combined collision, absorption, and track-length estimator from the MCNP calculations. The standard deviation (σ) represents the standard deviation of k_{eff} about the average combined collision, absorption, and track-length estimate due to the Monte Carlo calculation statistics. It should be noted that in the following sections, any reference to enrichment refers to assembly average initial enrichment, and burnup refers to assembly average burnup.

The corresponding MCNP input and output files for the cases used in this evaluation are provided electronically in Attachment IV.

6.1 MAXIMUM FRESH FUEL ENRICHMENT

This section presents the results of the maximum fresh fuel enrichments that can be loaded into the waste package with no burnup required. The determination of the maximum fresh fuel enrichment limit for the 44-BWR waste package with Ni-Gd Alloy absorber plates is determined by calculating k_{eff} for a range of initial enrichments and plotting them against the initial enrichments. The k_{eff} values plotted include a two- σ allowance for computational uncertainty. The intersection of this curve and a line representing the critical limit (or USL) shows where the waste package has a potential for criticality. The results of the fresh fuel calculations are presented in Table 15 for the preclosure and postclosure bounding configurations, and are illustrated in Figure 1.

Table 15. Fresh Fuel k_{eff} Results

Configuration Enrichment (Wt % U-235)	Preclosure Configuration			Postclosure Configuration		
	k_{eff}	σ	$k_{eff} + 2\sigma$	k_{eff}	σ	$k_{eff} + 2\sigma$
3.0	--	--	--	0.90045	0.00048	0.9017
3.5	0.90426	0.00051	0.90528	0.94246	0.00049	0.94405
4	0.93099	0.00057	0.93213	0.97904	0.00050	0.97751
4.5	0.95484	0.00055	0.95594	1.00672	0.00051	1.00726
5	0.97522	0.00052	0.97626	1.03234	0.00048	1.03289

A $CL (BU) = 0.980 - 0.0003 \cdot BU$ was taken from Moscalu (2004, p. 30) which is considered applicable to configuration class IP-1a from YMP (2003, Figure 3-2). Figure 1 illustrates that the maximum fresh fuel enrichment that would meet the loading curve criteria are 3.960 wt% U-235 for the preclosure configuration, and 3.999 wt% U-235 for the postclosure configuration.

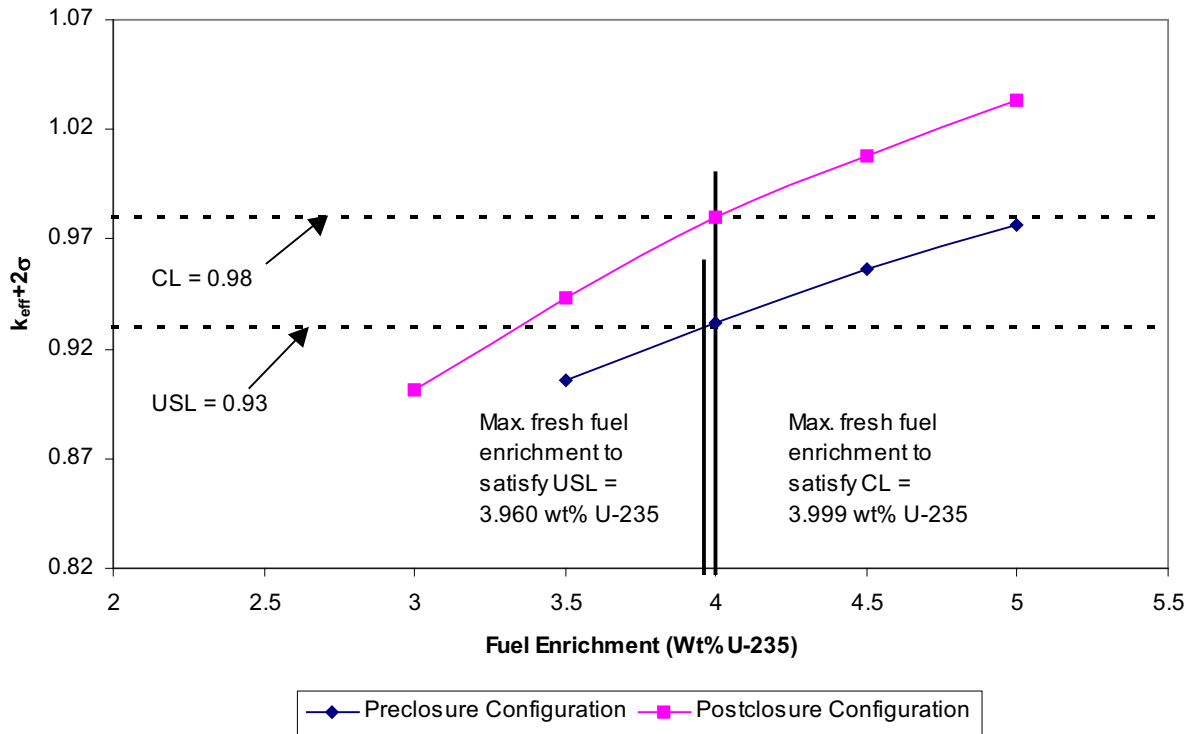


Figure 1. Fresh Fuel k_{eff} Results

6.2 BURNED FUEL

These cases used bounding spent nuclear fuel compositions that ensure that the Δk_{ISO} term from Equation 1 can be set to zero. The process for deriving spent fuel isotopics that set Δk_{ISO} to zero is discussed in BSC (2004j).

The results for spent fuel with five-year decay time (the five-year decay time is based on the minimum cooling time required for the fuel assemblies to be classified as standard fuel [10 CFR 961.11]) isotopic compositions are presented in Table 16. The postclosure irradiated fuel compositions were derived in Attachment IV (workbook *schoepite.xls*, sheet *SNF*). The minimum burnup required for each initial enrichment to meet the CL or USL is determined by plotting the calculated k_{eff} versus the burnup. The burnup value of the intersection of the plotted curve with the USL is the required minimum burnup. Any burnup value greater than this will result in a k_{eff} less than the CL or USL, and is acceptable to be loaded into the waste package. The results for the preclosure configuration 5.0 wt% U-235 initial enrichment cases are illustrated in Figure 2 which has an extrapolated minimum required burnup to meet the USL. In Figure 2 the USL is presented as a function of burnup with the USL equation provided in Table 17. The preclosure 3.5 to 4.5 wt% U-235 initial enriched cases were not plotted because they are below the USL at the minimum burnup that ensures Δk_{ISO} is set to zero. The postclosure cases were not plotted because they are

below the CL at the minimum burnup that ensures Δk_{ISO} is set to zero. The minimum burnups that ensure Δk_{ISO} is set to zero come from Wimmer (2004, Figure 34), and are provided in Table 18.

Table 16. Spent Nuclear Fuel k_{eff} Results

Initial Enrichment (Wt% U-235)	Burnup (GWd/ MTU)	Preclosure			Postclosure		
		k_{eff}	σ	$k_{eff}+2\sigma$	k_{eff}	σ	$k_{eff}+2\sigma$
3.5	10	0.87524	0.00051	0.87626	--	--	--
	15	0.86536	0.00051	0.86638	--	--	--
	20	0.84816	0.00052	0.84920	--	--	--
	25	0.83142	0.00048	0.83238	--	--	--
	30	0.81621	0.00048	0.81717	--	--	--
	35	0.80296	0.00056	0.80408	--	--	--
	40	0.78970	0.00052	0.79074	--	--	--
4.0	10	0.89266	0.00055	0.89376	0.92519	0.00045	0.92609
	15	0.88031	0.00055	0.88141	0.90865	0.00051	0.90967
	20	0.86251	0.00052	0.86355	0.88493	0.00049	0.88591
	25	0.84574	0.00056	0.84686	--	--	--
	30	0.82907	0.00049	0.83005	--	--	--
	35	0.81445	0.00047	0.81539	--	--	--
	40	0.80024	0.00053	0.80130	--	--	--
4.5	10	0.90795	0.00056	0.90907	0.94453	0.00049	0.94551
	15	0.89377	0.00055	0.89487	0.92687	0.00045	0.92777
	20	0.87522	0.00051	0.87624	0.90481	0.00049	0.90579
	25	0.85943	0.00056	0.86055	--	--	--
	30	0.84085	0.00049	0.84183	--	--	--
	35	0.82633	0.00044	0.82721	--	--	--
	40	0.81118	0.00050	0.81218	--	--	--
5.0	10	0.92162	0.00052	0.92266	0.96366	0.00047	0.96460
	15	0.90784	0.00054	0.90892	0.94440	0.00045	0.94530
	20	0.88907	0.00049	0.89005	0.92100	0.00050	0.92200
	25	0.87044	0.00052	0.87148	--	--	--
	30	0.85496	0.00052	0.85600	--	--	--
	35	0.83772	0.00052	0.83876	--	--	--
	40	0.82230	0.00050	0.82330	--	--	--

Table 17. Spent Nuclear Fuel Upper Limit Functions

Repository Period	Trend Parameter	Equation
Postclosure	Burnup	$CL (BU) = 0.980 - 0.0003 \cdot BU$
Preclosure	Burnup	$USL (BU) = 0.980 - 0.0003 \cdot BU - 0.05$

NOTE: Moscalu (2004, p. 30) provides the CL function which is transformed into an USL function using $\Delta k_m = 0.05$ (see Section 5 for details of USL transformation)

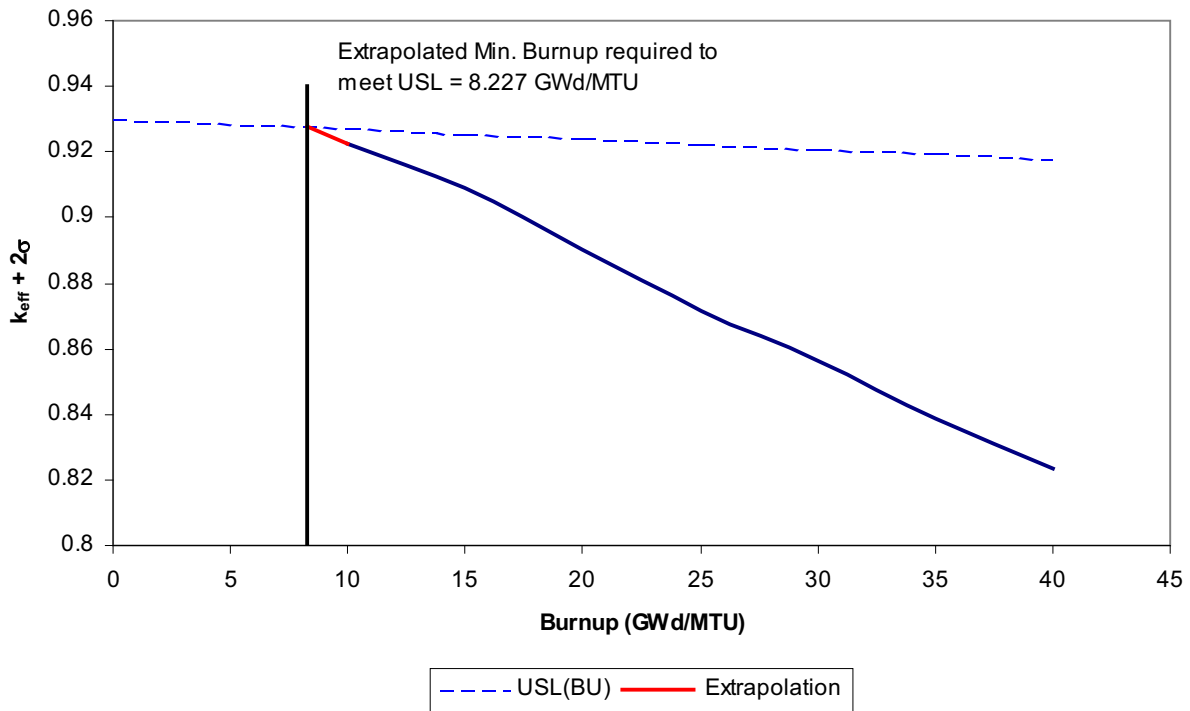


Figure 2. Spent Nuclear Fuel k_{eff} Results for 5.0 Wt% U-235 Initial Enrichment

For generating the loading curve initial enrichments greater than 3.960 wt% U-235 (see Figure 1) will require burnup credit in order to remain at or below the USL, and enrichments greater than 3.999 for the CL. Wimmer (2004, Figure 34) illustrates that the minimum burnup required to set Δk_{ISO} to zero is 10.3 GWd/MTU for 4.0 wt% U-235 initial enriched fuel assemblies, which can also be used as the minimum for enrichments greater than 3.960 wt% U-235. Based on the results presented in Table 16, the minimum burnups from Wimmer (2004, Figure 34) will result in k_{eff} values below the USL and CL and will be used in establishing the loading curve.

The minimum required burnups as a function of initial enrichment are presented in Table 18. Also, an additional margin for a burnup uncertainty of five percent is included.

Table 18. Minimum Required Burnups for Intercept of Upper Subcritical Limit

Initial Enrichment (Wt% U-235)	Burnup (GWd/MTU) ^a	5% BU Unc. ^b
3.960	0	0
4.0	10.3	10.82
4.5	18.45 ^c	19.37
5.0	26.6	27.93

NOTES: ^a Values are minimums from Wimmer 2004, Figure 34, to ensure conservative isotopic compositions
^b Required minimum burnup including 5% uncertainty associated with assembly burnup records
^c Interpolated from 4.0 and 5.0 wt% U-235 minimum values

6.3 WASTE STREAM COMPARISON

The waste stream inventory in terms of number of fuel assemblies at given burnups and enrichments was taken from CRWMS M&O (2000, Attachment III) using the "Case A" arrival forecast. "Case A" refers to 10-year-old youngest fuel first for 63,000 MTU. This arrival forecast was selected based on Licensing Position LP-009, *Waste Stream Parameters* (Williams 2003). The results of the loading curve compared against the waste stream inventory are presented in Figure 3.

The squares in the legend indicate number groupings of assemblies at a particular burnup and enrichment (e.g., 100-199 indicates that there are 100 to 199 assemblies at a listed burnup and enrichment); *Nominal LC* is the loading curve based on the nominal required minimum burnup; and *5% BU Unc. LC* is the loading curve adjusted to accommodate five percent uncertainty associated with the reported assembly burnups. The waste stream information that was extracted and sorted is provided in Attachment IV as the workbook *wstreamplot.xls*.

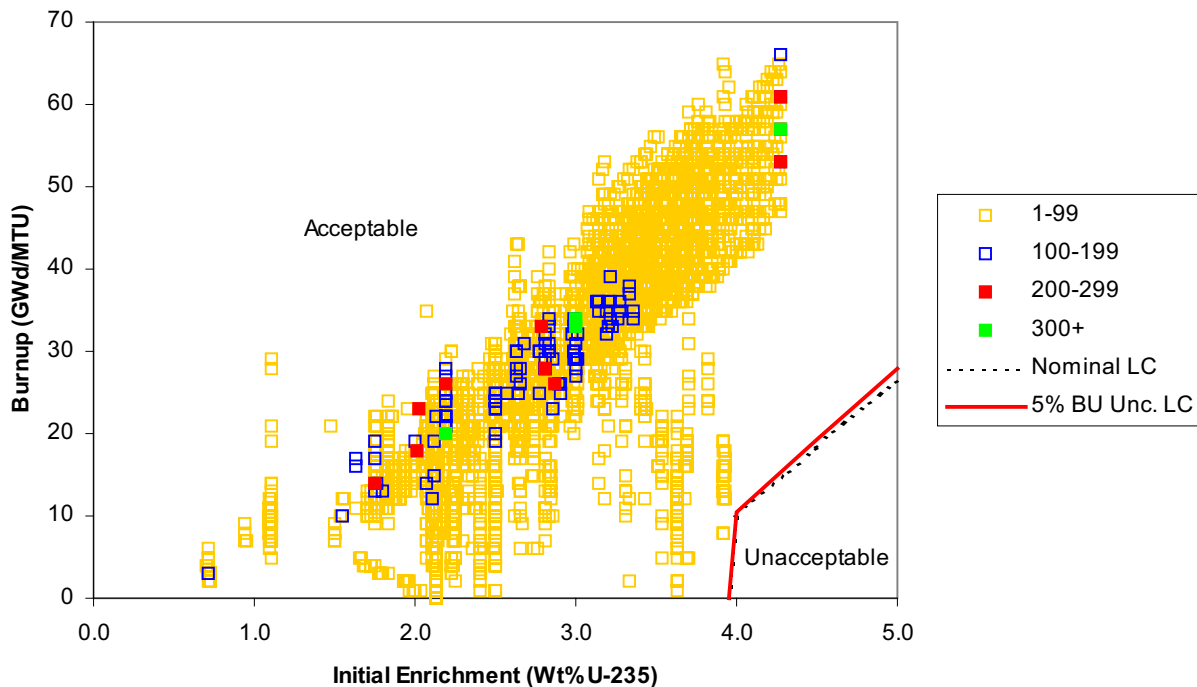


Figure 3. Loading Curve and Projected Waste Stream

6.4 SUMMARY OF RESULTS

Results presented in Attachment I (Table 26) illustrate that the 44-BWR waste package with Ni-Gd Alloy absorber plates will not go critical with commercial fuel assemblies if there is no moderator present within the waste package.

In equation notation the loading curve is as shown in Equation 11:

$$\begin{aligned}
 BU &= 270.375 * E - 1070.69 \quad (3.960 \text{ wt\% U-235} < E \leq 4.0 \text{ wt\% U-235}) \\
 BU &= 17.115 * E - 57.645 \quad (4.0 \text{ wt\% U-235} < E \leq 5.0 \text{ wt\% U-235})
 \end{aligned}
 \tag{Eq. 11}$$

The results of this report allow 100 percent of the current BWR projected waste stream to be disposed of in the 44-BWR waste package with Ni-Gd Alloy absorber plates.

All outputs are reasonable compared to the inputs and the results of this calculation are suitable for their intended use.

7. REFERENCES

10 CFR (Code of Federal Regulations) 63. Energy: Disposal of High-Level Radioactive Wastes in a Geologic Repository at Yucca Mountain, Nevada. Readily available.

10 CFR (Code of Federal Regulations) 961. Energy: Standard Contract for Disposal of Spent Nuclear Fuel and/or High-Level Radioactive Waste. Readily Available.

ASM International 1967. "Zircaloy-2, Nuclear Reactor Alloy, Filing Code:Zr-3 Zirconium Alloy." *Alloy Digest*, (July), . Materials Park, Ohio: ASM International. TIC: 239929.

ASM International. 1987. *Corrosion*. Volume 13 of *Metals Handbook*. 9th Edition. Metals Park, Ohio: ASM International. TIC: 209807.

ASM International 1990. *Properties and Selection: Nonferrous Alloys and Special-Purpose Materials*. Volume 2 of *ASM Handbook*. Formerly 10th Edition, Metals Handbook. 5th Printing 1998. [Materials Park, Ohio]: ASM International. TIC: 241059.

ASME (American Society of Mechanical Engineers) 2001. *2001 ASME Boiler and Pressure Vessel Code (includes 2002 addenda)*. New York, New York: American Society of Mechanical Engineers. TIC: 251425.

ASTM A 516/A 516M-90. 1991. *Standard Specification for Pressure Vessel Plates, Carbon Steel, for Moderate-and Lower-Temperature Service*. West Conshohocken, Pennsylvania: American Society for Testing and Materials. TIC: 240032.

ASTM B 811-97. 2000. *Standard Specification for Wrought Zirconium Alloy Seamless Tubes for Nuclear Reactor Fuel Cladding*. West Conshohocken, Pennsylvania: American Society for Testing and Materials. TIC: 247245.

ASTM B 932-04. 2004. *Standard Specification for Low-Carbon Nickel-Chromium-Molybdenum-Gadolinium Alloy Plate, Sheet, and Strip*. West Conshohocken, Pennsylvania: American Society for Testing and Materials. TIC: 255846.

ASTM G 1-90 (Reapproved 1999). 1999. *Standard Practice for Preparing, Cleaning, and Evaluating Corrosion Test Specimens*. West Conshohocken, Pennsylvania: American Society for Testing and Materials. TIC: 238771.

Audi, G. and Wapstra, A.H. 1995. *Atomic Mass Adjustment, Mass List for Analysis*. [Upton, New York: Brookhaven National Laboratory, National Nuclear Data Center]. TIC: 242718.

Bowman, S.M.; Hermann, O.W.; and Brady, M.C. 1995. *Sequoyah Unit 2 Cycle 3*. Volume 2 of *Scale-4 Analysis of Pressurized Water Reactor Critical Configurations*. ORNL/TM-12294/V2. Oak Ridge, Tennessee: Oak Ridge National Laboratory. TIC: 244397.

Briesmeister, J.F., ed. 1997. *MCNP-A General Monte Carlo N-Particle Transport Code*. LA-12625-M, Version 4B. Los Alamos, New Mexico: Los Alamos National Laboratory. ACC: MOL.19980624.0328.

BSC (Bechtel SAIC Company) 2002. *External Criticality Calculation for DOE SNF Codisposal Waste Packages*. CAL-DSD-NU-000001 REV A. Las Vegas, Nevada: Bechtel SAIC Company. ACC: MOL.20021105.0162.

BSC (Bechtel SAIC Company) 2003. *Design and Engineering Organization, 44-BWR Waste Package Configuration*. 000-MW0-DSU0-00502-000-00A. Las Vegas, Nevada: Bechtel SAIC Company. ACC: ENG.20031021.0004.

BSC (Bechtel SAIC Company) 2004a. *Design and Engineering, 44 BWR Side Guide*. 000-MW0-DSU0-01501-000-00A. Las Vegas, Nevada: Bechtel SAIC Company. ACC: ENG.20040305.0004.

BSC (Bechtel SAIC Company) 2004b. *Design and Engineering, 44 BWR Corner Guide*. 000-MW0-DSU0-01601-000-00A. Las Vegas, Nevada: Bechtel SAIC Company. ACC: ENG.20040303.0052.

BSC (Bechtel SAIC Company) 2004c. *44 BWR A, B, D, F & G Fuel Plates*. 000-MW0-DSU0-01801-000-00B. Las Vegas, Nevada: Bechtel SAIC Company. ACC: ENG.20040804.0002.

BSC (Bechtel SAIC Company) 2004d. *44 BWR C & E Fuel Plates*. 000-MW0-DSU0-01901-000-00B. Las Vegas, Nevada: Bechtel SAIC Company. ACC: ENG.20040804.0003.

BSC (Bechtel SAIC Company) 2004e. *44-BWR Waste Package Configuration*. 000-MW0-DSU0-00503-000-00C. Las Vegas, Nevada: Bechtel SAIC Company. ACC: ENG.20040708.0007.

BSC (Bechtel SAIC Company) 2004f. *Geochemistry Model Abstraction and Sensitivity Studies for the 21 PWR CSNF Waste Packages*. MDL-DSU-MD-000001 REV 00 [Errata 001]. Las Vegas, Nevada: Bechtel SAIC Company. ACC: MOL.20021107.0154; DOC.20040225.0005.

BSC (Bechtel SAIC Company) 2004g. *Seismic Consequence Abstraction*. MDL-WIS-PA-000003 REV 0 Errata 1. Las Vegas, Nevada: Bechtel SAIC Company. ACC: DOC.20030818.0006; DOC.20040218.0002.

BSC (Bechtel SAIC Company) 2004h. *Design and Engineering, Fuel Tube*. 000-MW0-DSU0-02001-000-00A. Las Vegas, Nevada: Bechtel SAIC Company. ACC: ENG.20040305.0012.

BSC (Bechtel SAIC Company) 2004i. *Q-List*. 000-30R-MGR0-00500-000-000 REV 00. Las Vegas, Nevada: Bechtel SAIC Company. ACC: ENG.20040721.0007.

BSC (Bechtel SAIC Company) 2004j. *Isotopic Model for Commercial SNF Burnup Credit*. CAL-DSU-NU-000007 REV 00A. Las Vegas, Nevada: Bechtel SAIC Company. ACC: DOC.20040818.0001.

Title: 44-BWR Waste Package Loading Curve Evaluation

Document Identifier: CAL-DSU-NU-000008 REV 00A

Page 32 of 34

Canori, G.F. and Leitner, M.M. 2003. *Project Requirements Document*. TER-MGR-MD-000001 REV 02. Las Vegas, Nevada: Bechtel SAIC Company. ACC: DOC.20031222.0006.

CRWMS M&O 1998a. *Software Qualification Report for MCNP Version 4B2, A General Monte Carlo N-Particle Transport Code*. CSCI: 30033 V4B2LV. DI: 30033-2003, Rev. 01. Las Vegas, Nevada: CRWMS M&O. ACC: MOL.19980622.0637.

CRWMS M&O 1998b. *Software Code: MCNP*. V4B2LV. HP, HPUX 9.07 and 10.20; PC, Windows 95; Sun, Solaris 2.6. 30033 V4B2LV.

CRWMS M&O 1998c. *Selection of MCNP Cross Section Libraries*. B00000000-01717-5705-00099 REV 00. Las Vegas, Nevada: CRWMS M&O. ACC: MOL.19980722.0042.

CRWMS M&O 2000. *Waste Packages and Source Terms for the Commercial 1999 Design Basis Waste Streams*. CAL-MGR-MD-000001 REV 00. Las Vegas, Nevada: CRWMS M&O. ACC: MOL.20000214.0479.

DOE (U.S. Department of Energy) 2004. *Quality Assurance Requirements and Description*. DOE/RW-0333P, Rev. 16. Washington, D.C.: U.S. Department of Energy, Office of Civilian Radioactive Waste Management. ACC: DOC.20040823.0004.

Doraswamy, N. 2004. *Project Design Criteria Document*. 000-3DR-MGR0-00100-000-002. Las Vegas, Nevada: Bechtel SAIC Company. ACC: ENG.20040721.0003.

Einziger, R.E. 1991. "Effects of an Oxidizing Atmosphere in a Spent Fuel Packaging Facility." *Proceedings of the Topical Meeting on Nuclear Waste Packaging, FOCUS '91, September 29–October 2, 1991, Las Vegas, Nevada*. Pages 88-99. La Grange Park, Illinois: American Nuclear Society. TIC: 231173.

Gelest, Inc. 2004. *Gelest Silicone Fluids : Stable, Inert Media*. Morrisville, Pennsylvania: Gelest, Inc. TIC: 256122.

GS000308313211.001. Geochemistry of Repository Block. Submittal date: 03/27/2000.

Harwell, J.W. 2003. *Commercial Reactor Reactivity Analysis for Grand Gulf, Unit 1*. 32-5029393-00. [Lynchburg, Virginia]: Framatome ANP. ACC: DOC.20040109.0003.

Larsen, N.H.; Parkos, G.R.; and Raza, O. 1976. *Core Design and Operating Data for Cycles 1 and 2 of Quad Cities 1*. EPRI NP-240. Palo Alto, California: Electric Power Research Institute. TIC: 237267.

LB990501233129.001. Fracture Properties for the UZ Model Grids and Uncalibrated Fracture and Matrix Properties for the UZ Model Layers for AMR U0090, "Analysis of Hydrologic Properties Data". Submittal date: 08/25/1999.

Lide, D.R., ed. 2002. *CRC Handbook of Chemistry and Physics*. 83rd Edition. Boca Raton, Florida: CRC Press. TIC: 253582.

LP-SI.11Q-BSC, Rev. 0, ICN 0. *Software Management*. Washington, D.C.: U.S. Department of Energy, Office of Civilian Radioactive Waste Management. ACC: DOC.20040225.0007.

Moscalu, D.R. 2004. *Range of Parameters for BWR SNF in a 44-BWR Waste Package*. 32-5041139-00. Las Vegas, Nevada: Areva. ACC: DOC.20040623.0004.

MO0003RIB00071.000. Physical and Chemical Characteristics of Alloy 22. Submittal date: 03/13/2000.

MO0109HYMXP.001. Matrix Hydrologic Properties Data. Submittal date: 09/17/2001.

NRC (U.S. Nuclear Regulatory Commission) 2000. *Standard Review Plan for Spent Fuel Dry Storage Facilities*. NUREG-1567. Washington, D.C.: U.S. Nuclear Regulatory Commission. TIC: 247929.

Parrington, J.R.; Knox, H.D.; Breneman, S.L.; Baum, E.M.; and Feiner, F. 1996. *Nuclides and Isotopes, Chart of the Nuclides*. 15th Edition. San Jose, California: General Electric Company and KAPL, Inc. TIC: 233705.

Punatar, M.K. 2001. *Summary Report of Commercial Reactor Criticality Data for Grand Gulf Unit 1*. TDR-UDC-NU-000002 REV 00. Las Vegas, Nevada: Bechtel SAIC Company. ACC: MOL.20011008.0008.

Roberts, W.L.; Campbell, T.J.; and Rapp, G.R., Jr. 1990. *Encyclopedia of Minerals*. 2nd Edition. New York, New York: Van Nostrand Reinhold. TIC: 242976.

Todreas, N.E. and Kazimi, M.S. 1990. *Nuclear Systems I, Thermal Hydraulic Fundamentals*. New York, New York: Hemisphere Publishing. TIC: 226511.

Williams, N.H. 2003. "Contract No. DE-AC28-01RW12101 - Licensing Position-009, Waste Stream Parameters." Letter from N.H. Williams (BSC) to J.D. Ziegler (DOE/ORD), November 13, 2003, 1105039412, with enclosure. ACC: MOL.20031215.0076.

Williams, N.H. 2004. *Decision Proposal, Technical Decision, Statement for Consideration: Change the Current Neutron Absorber Material in the CSNF Waste Packages from Borated Stainless Steel to a Nickel-Gadolinium Alloy*. Tracking No. TMRB-2004-009. [Las Vegas, Nevada: Bechtel SAIC Company]. ACC: MOL.20040622.0307.

Wimmer, L.B. 2004. *Isotopic Generation and Confirmation of the BWR Appl. Model*. 32-5035847-01. Las Vegas, Nevada: Areva. ACC: DOC.20040630.0007.

YMP (Yucca Mountain Site Characterization Project) 2003. *Disposal Criticality Analysis Methodology Topical Report*. YMP/TR-004Q, Rev. 02. Las Vegas, Nevada: Yucca Mountain Site Characterization Office. ACC: DOC.20031110.0005.

8. ATTACHMENTS

Table 19 presents the attachment specifications for this calculation file.

Table 19. Attachment Listing

Attachment #	# of Pages	Date Created	Description
I	14	N/A	Sensitivity studies
II	6	N/A	Alternative neutron absorber evaluation
III	2	N/A	Listing of contents on Attachment IV
IV	N/A	06/15/2004	Compact Disc attachment containing information listed in Attachment III

Attachment I: Sensitivity Studies

I. DESCRIPTION AND RESULTS

Sensitivity studies were performed to observe the waste package as it behaves over time in the repository and to determine which material characteristics result in the highest k_{eff} values. A brief description of the sensitivity studies performed and their results is provided in the following sections.

In each of the sensitivity cases, the waste package dimensions correspond to those provided in Attachment IV (*44BWRWP.zip*). Each configuration is represented with dry tuff surrounding the waste package. The dry tuff composition for each of the sensitivity cases is represented as having a porosity of 15.7 % (BSC 2002, p. 10) and a tuff composition as listed in Table 20.

Table 20. Tuff Composition for Sensitivity Cases

Compound	Wt%
SiO ₂	76.83
Al ₂ O ₃	12.74
FeO	0.84
MgO	0.25
CaO	0.56
Na ₂ O	3.59
K ₂ O	4.93
TiO ₂	0.1
P ₂ O ₅	0.02
MnO	0.07

Source: BSC 2002, Table 5-3.

NOTE: Derived elemental/isotopic number densities for MCNP inputs are provided in Attachment IV, spreadsheet *Tuff composition.xls*, sheet *Sens_tuff*

I.1 ASSEMBLY LATTICE

Variations in fuel assembly lattice design were evaluated. This set of cases was performed in order to assess which fuel assembly lattice design would result in the highest k_{eff} values when loaded in a waste package configuration and confirm Assumption 3.1. Fuel assembly lattices were varied using 7x7, 8x8, and 9x9 geometric arrangements in pure water. The 8x8 and 9x9 base assembly design parameters were taken from Punatar (2001, Sections 2 and 3). The 8x8 design was evaluated with 2 water rods, 4 water rods, 4 lattice cells containing only water (which is consistent with 1 large water rod), and the 9x9 design was evaluated with 5 water rods. The 7x7 fuel assembly design parameters are from Larsen et. al. (1976). These cases were evaluated using a fresh fuel enrichment of 5.0 wt% U-235 in a nominal waste package configuration. The results of this set of cases are presented in Table 23 and illustrated in Figure 4. The channel and upper and lower tie plate region compositions as derived in Attachment IV (spreadsheet *GEassembly_Vol.xls*) were maintained for each of the designs, as well as the fuel pellet density.

Table 21. 8x8 and 9x9 BWR Fuel Assembly Specifications

Assembly Component	Specification	
	8x8	9x9
Lattice	8x8	9x9
Fuel Pellet Outer Diameter ^a	1.02997 cm	N/A
Fuel Rod Cladding Inner Diameter	1.05156 cm	0.95008 cm ^b
Fuel Rod Cladding Outer Diameter	1.22936 cm	1.10136 cm ^b
Number of Water Rods	2	5
Channel Inner Width	13.246 cm	13.246 cm
Channel Thickness	0.3048 cm	0.3048 cm
Active Fuel Length	381 cm	381 cm
Clad Material	Zircaloy-2	Zircaloy-2
Channel Material	Zircaloy-2	Zircaloy-2
Pin Pitch	1.61544 cm	1.43002 cm

Source: Punatar 2001, Section 2

NOTES: ^a The base case representations use a smeared pellet density over the inner clad diameter.
^b Values were averaged and taken directly from Harwell (2003, case *mcnp20*, assembly K2)

Table 22. 7x7 BWR Fuel Assembly Specifications

Assembly Component	Specification
	7x7
Lattice	7x7
Fuel Pellet Outer Diameter ^a	1.23952 cm (0.488 in.) ^b
Fuel Rod Cladding Thickness	0.08128 cm (0.032 in.)
Fuel Rod Cladding Inner Diameter	1.26746 cm
Fuel Rod Cladding Outer Diameter	1.43002 cm (0.563 in.)
Active Fuel Length	365.76 cm (144 in.)
Clad Material	Zircaloy-2
Channel Material	Zircaloy-2
Pin Pitch	1.87452 cm (0.738 in.)
Channel Inner Width ^c	13.246 cm
Channel Thickness ^c	0.3048 cm

Source: Larsen et. al. 1976, pp. A-1 to A-3

NOTES: ^a The base case representations use a smeared pellet density over the inner clad diameter.
^b Values in parentheses are from the source reference.
^c Channel dimensions were taken from Punatar 2001, Table 2-1.

Table 23. Fuel Assembly Lattice Design k_{eff} Results

Assembly Description	Designation	Filename	k_{eff}	σ
8x8 with 2 water rods	8x8 2WR	8x8wr2	0.95385	0.00056
7x7	7x7	7x7	0.96562	0.00057
8x8 with 4 water rods	8x8 4WR	8x8wr4	0.95447	0.00053
9x9 with 5 water rods	9x9 5WR	9x9	0.95597	0.0005
8x8 with 4 empty cells in center for water (representative of 1 big water rod)	8x8 1LGWR	8x8wr1B	0.95838	0.00057

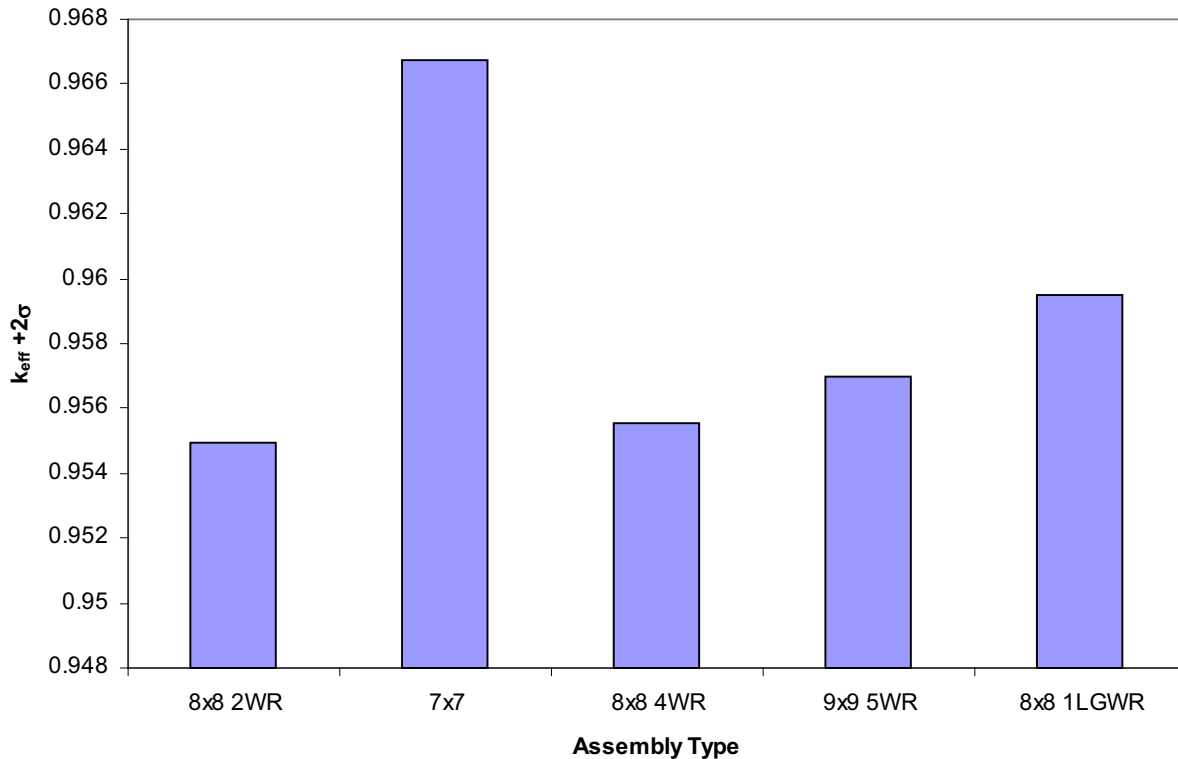


Figure 4. Fuel Assembly Lattice Design k_{eff} Results

Based on the results presented in Table 23 and Figure 4, the representation for the 7x7 assembly produces the highest k_{eff} .

I.2 FUEL DENSITY EFFECTS

Variations in fuel density were evaluated. Two sets of cases were evaluated with the 8x8 assembly design with 2 water rods - smeared and unsmeared. This set of cases was performed in order to assess the fuel density that would result in the highest k_{eff} values given the fixed lattice dimensions of the fuel assembly and maintaining the assembly mass. Fuel density values were varied from 9.78 g/cm³ through 10.696 g/cm³ for a representative assembly with 5.0 wt% U-235 fresh fuel. The results of this set of cases are presented in Table 24 and illustrated in Figure 5.

Table 24. Fuel Density k_{eff} Results

Smeared				Unsmeared			
Fuel Density (g/cm ³)	k_{eff}	σ	Filename	Fuel Density (g/cm ³)	k_{eff}	σ	Filename
9.78 ^a	0.95385	0.00056	8x8wr2	9.896	0.95157	0.00052	d9
9.88	0.95549	0.00057	d2	9.996	0.95143	0.00052	d8
9.98	0.95684	0.00059	d3	10.096	0.95200	0.00055	d7
10.08	0.95892	0.00053	d4	10.196 ^a	0.95325	0.00051	d1
10.18	0.95877	0.00053	d5	10.296	0.95513	0.00053	d2
10.28	0.95945	0.00056	d6	10.396	0.95689	0.00053	d3

Table 24. Fuel Density k_{eff} Results

Smeared				Unsmeared			
Fuel Density (g/cm ³)	k_{eff}	σ	Filename	Fuel Density (g/cm ³)	k_{eff}	σ	Filename
10.38	0.96121	0.00059	d7	10.496	0.95781	0.00048	d4
10.48	0.96269	0.00052	d8	10.596	0.95862	0.00057	d5
10.58	0.96228	0.00058	d9	10.696	0.95909	0.00057	d6
				10.196 ^{a, b}	0.95855	0.00056	d0

NOTES: ^a Cases maintained equal mass of UO₂
^b MCNP representation had water filling gap between fuel and clad, this configuration is considered nonmechanistic for any extended period of time since the fuel material would oxidize and hydrate forming configurations similar to Section I.8

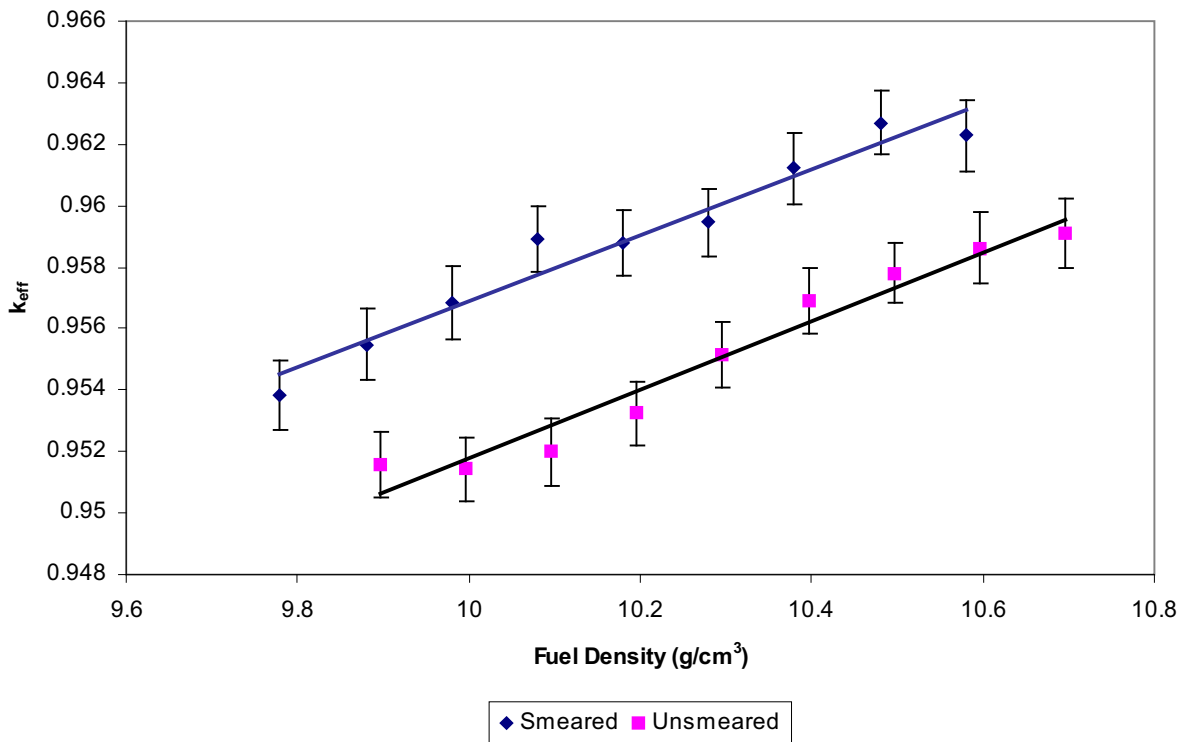


Figure 5. Fuel Density k_{eff} Results

I.3 WASTE PACKAGE FUEL ASSEMBLY GEOMETRY

Variations in waste package fuel assembly geometry were evaluated. This set of cases investigated the effects of different positioning of the fuel assemblies within the waste package. Three configurations were evaluated using the 7x7 assembly design. One where the assembly was centered within the waste package basket cell as could occur when the waste package is in a vertical position during loading operations, and two where the fuel assemblies are resting against the basket plates which occurs when the waste package is in a horizontal position. The three different geometric representations are provided in Figures 6 through 8 and the results presented in Table 25. Base case fresh fuel compositions correspond to a fuel assembly with 5.0 wt% U-235 initial enrichment.

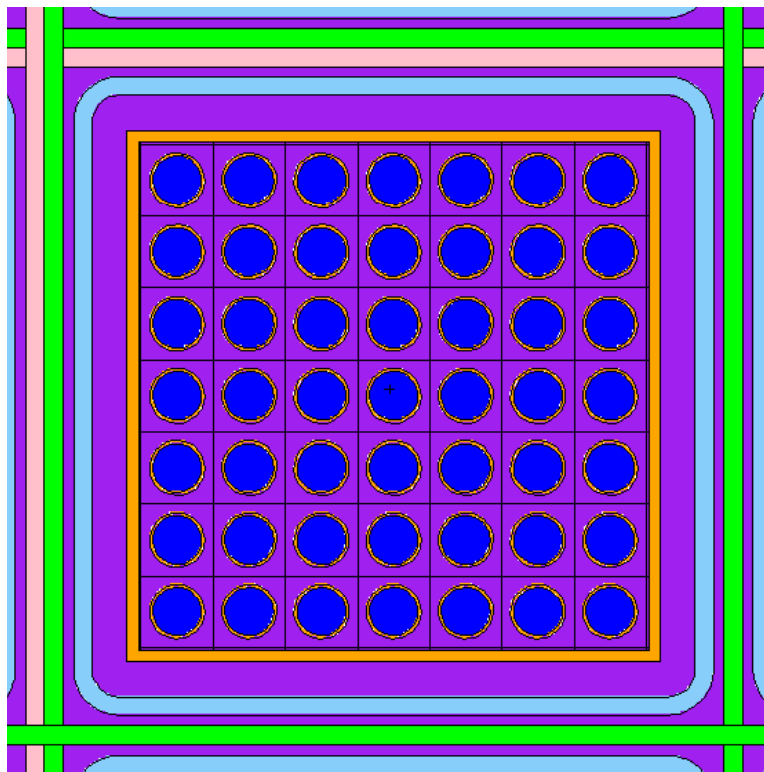


Figure 6. Standard Vertical Position Waste Package Geometry

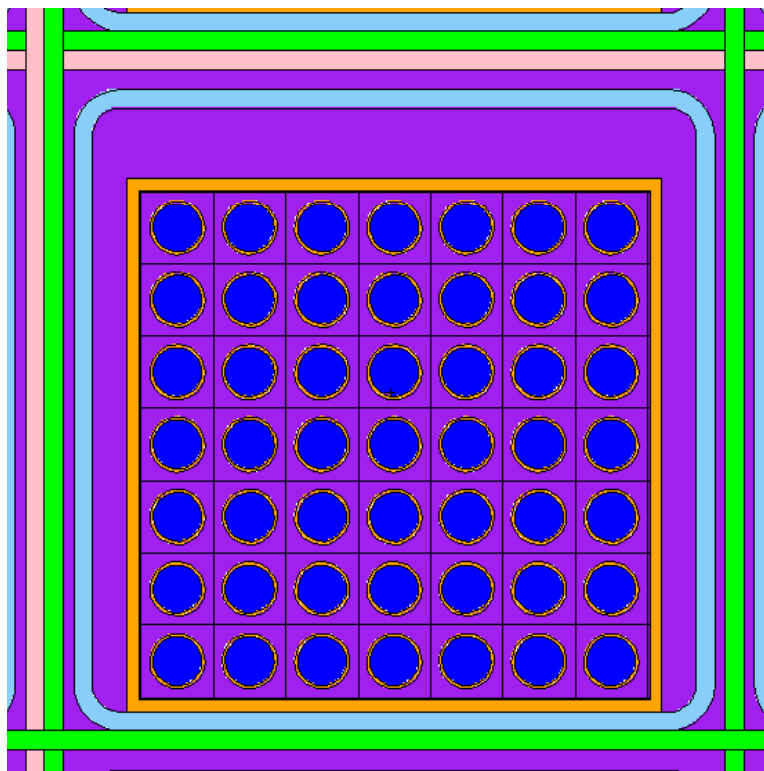


Figure 7. Standard Horizontal Position Waste Package Geometry

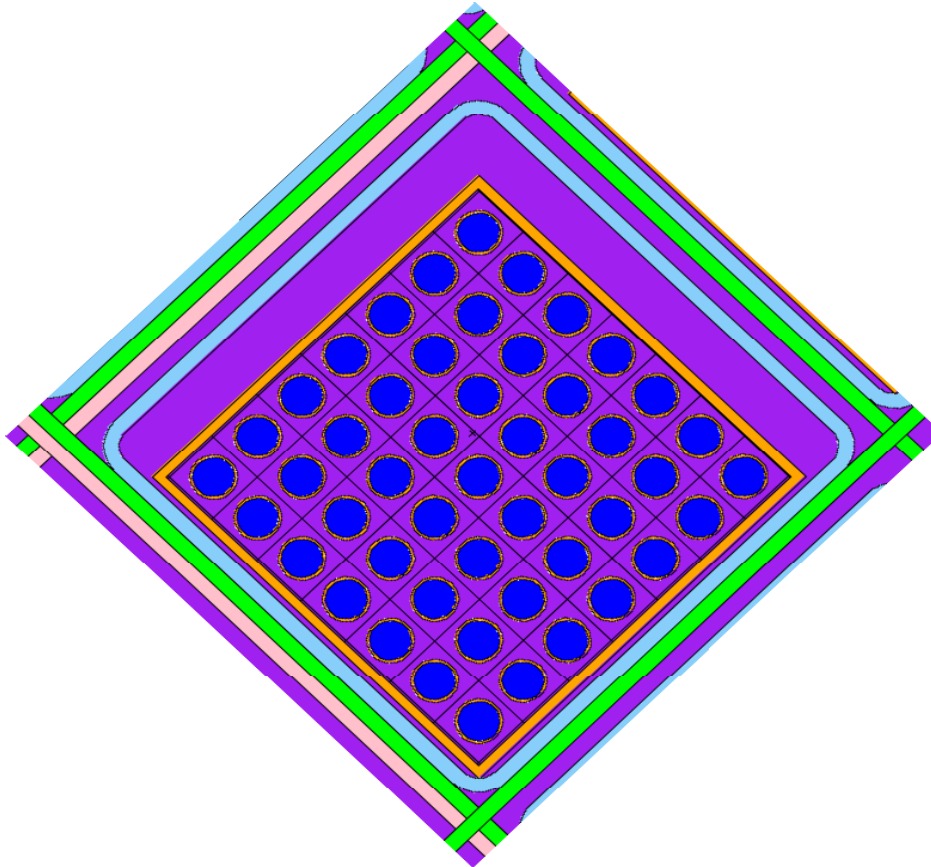


Figure 8. Rotated Horizontal Position Waste Package Geometry

Table 25. Fuel Assembly Geometry k_{eff} Results

Configuration	k_{eff}	σ	Filename
Standard Vertical	0.96562	0.00057	7x7
Standard Horizontal	0.95214	0.00054	horiz1
Rotated Horizontal	0.95162	0.00056	h2full

Based on the results presented in Table 25 the standard vertical waste package geometry results in the highest k_{eff} .

I.4 OPTIMUM MODERATOR DENSITY

A search for optimum moderator density was performed. This set of cases was used to show that the fuel assemblies placed into a waste package configuration is an under-moderated system. Moderator density values were varied from 0.0 g/cm³ through 1.0 g/cm³. Base case values correspond to a fresh fuel assembly with 5.0 wt% U-235 initial enrichment. The results of this set of cases are presented in Table 26 and are illustrated in Figure 9.

Table 26. Moderator Density Sensitivity Results

Moderator Density (g/cm ³)	k _{eff}	σ	Filename
0.0	0.40131	0.00018	case0
0.1	0.59716	0.00037	case1
0.2	0.69781	0.00041	case2
0.3	0.76799	0.00044	case3
0.4	0.82015	0.0005	case4
0.5	0.86029	0.00052	case5
0.6	0.88941	0.00051	case6
0.7	0.91526	0.00054	case7
0.8	0.93532	0.00051	case8
0.9	0.95149	0.00056	case9
1.0	0.96562	0.00057	7x7

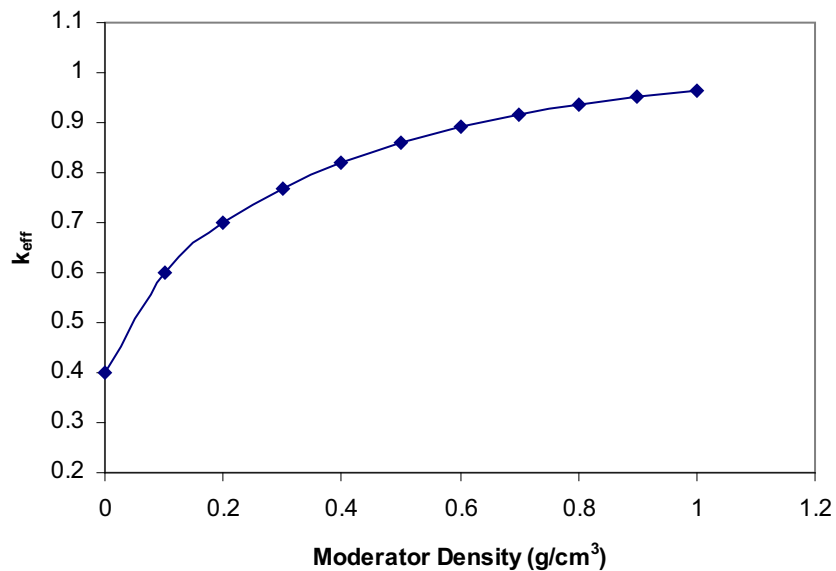
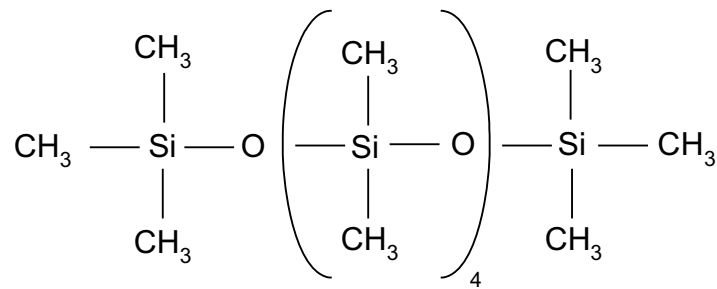


Figure 9. Moderator Density Sensitivity Results

Another moderator material was evaluated instead of water. Hydraulic fluid/oil that may leak from a handling crane. Estimates indicate that a 100 ton or 200 ton crane, which could be utilized by the handling facility, would contain approximately 100 to 135 gallons of fluid/oil. The representative hydraulic fluid follows the description provided in Gelest, inc. (2004) and the material safety data sheet contained in Attachment IV (0130223.pdf) and has a chemical form as follows:



Source: Gelest Inc. 2004, p. 11

For the event of this fluid/oil getting into the waste package several cases were evaluated to observe the effects on system reactivity. The cases were as follows:

Case1 - the entire waste package is filled with fluid/oil (limited quantity indicates this is non-mechanistic, but will bound all other configurations ($k_{\text{eff}} = 0.91226$, $\sigma = 0.00054$))

In order to assess whether the hydraulic fluid results in an over- or under-moderation of the system, the density of the material was lowered in these cases to observe the effects on k_{eff} :

Case2 - used a density of 0.85 g/cm^3 ($k_{\text{eff}} = 0.90315$, $\sigma = 0.00050$)

Case3 - used a density of 0.8 g/cm^3 ($k_{\text{eff}} = 0.89414$, $\sigma = 0.00052$)

Since the resulting k_{eff} values decreased with decreased density, the system is under-moderated and no further evaluations are warranted. Water is a better moderator than the representative hydraulic fluid.

1.5 SIMPLIFIED GEOMETRY

Several geometric simplifications were evaluated in order to determine the impact on system reactivity. An external trunion region and basket stiffeners are present on the drawings presented in Attachment IV (*44BWRWP.zip*). A comparison was made between cases with and without the trunion region as well as with and without the stiffeners being represented. Configurations were evaluated using the 7x7 assembly design with 5.0 wt% U-235 fresh fuel. The results of this set of cases are presented in Table 27.

Table 27. Simplified Geometry Results

Case Description	k_{eff}	σ	Filename
Base case with no trunion region and basket stiffeners present	0.96562	0.00057	7x7
Base case with trunion region and basket stiffeners present	0.96524	0.00053	7x7wt
Base case with no trunion region and no stiffeners present	0.96731	0.00055	7x7wo

These results indicate that the presence of trunions or stiffeners in the representation have an insignificant impact on system reactivity.

I.6 TUFF EVALUATIONS

Variations for tuff present in and around the waste package were evaluated. This set of cases was performed in order to assess the impact tuff could have on system reactivity. Various levels of saturation were evaluated, as well as geometric arrangements. Configurations were evaluated using the 7x7 assembly design with 5.0 wt% U-235 fresh fuel. The results for the external tuff set of cases are presented in Table 28. Cases where the tuff material was uniformly dispersed within the waste package, but external to the channel are presented in Table 29. This set of cases is very unlikely since the basket plates would serve as a barrier to prevent tuff from getting into the internal regions of the basket geometry, and there is no mechanism to keep water only in the inside of the channels. Also, if tuff could migrate to the inside of the basket geometry, then it would be able to get into the channel area, where it would exclude moderator, and thus reduce k_{eff} . Cases where the tuff would most likely accumulate (in the external regions of the basket geometry) were evaluated and the results are presented in Table 30.

Table 28. External Waste Package Tuff Evaluation Results

Case Description	k_{eff}	σ	Filename
Dry tuff outside waste package	0.96562	0.00057	7x7
100% saturated tuff outside waste package	0.96606	0.00052	tuffsat
Water outside waste package	0.96611	0.00054	7x7wr
Void outside waste package	0.96688	0.00054	7x7vr

Table 29. Waste Package Tuff Internal Configuration 1 Evaluation Results

Case Description	k_{eff}	σ	Filename
Dry tuff in all void regions	0.47835	0.00021	t0all
100% saturated tuff in all void regions	0.69185	0.00041	t100all
Dry tuff in all void regions external to channel which contains pure water	1.09382	0.00053	tuff
25% saturated tuff in all void regions external to channel which contains pure water	1.08553	0.00059	tuff25
50% saturated tuff in all void regions external to channel which contains pure water	1.07713	0.00051	tuff50
75% saturated tuff in all void regions external to channel which contains pure water	1.07181	0.00045	tuff75
100% saturated tuff in all void regions external to channel which contains pure water	1.06412	0.00050	tuff100

The final four cases in Table 29 are non-mechanistic but are presented for illustrative purposes only.

Table 30. Waste Package Tuff Internal Configuration 2 Evaluation Results

Case Description	k_{eff}	σ	Filename
Dry tuff in all outer regions, pure water in inner regions	0.97752	0.00052	tout1
25% saturated tuff in all outer regions, pure water in inner regions	0.97435	0.00054	tout2
50% saturated tuff in all outer regions, pure water in inner regions	0.97381	0.00055	tout3
75% saturated tuff in all outer regions, pure water in inner regions	0.97225	0.00056	tout4
100% saturated tuff in all outer regions, pure water in inner regions	0.97279	0.00054	tout5

These results indicate that a dry tuff reflector inside the package and around the fuel assemblies with water inside the channels produces the highest k_{eff} . This case is non-mechanistic as that tuff that accumulates in the waste package would be mobile and reach a configuration similar to that described by case *t100all*, which results in a very low k_{eff} . Therefore, tuff accumulation inside the waste package is considered non-mechanistic.

I.7 ABSORBER PLATE DEGRADATION

A series of cases were evaluated in order to determine the effects of the absorber plate as it degrades over time. Variations were made to the amount of corrosion product retained within the basket cells to observe the sensitivity of neutron spectrum. The corrosion product mixture composition was derived in Attachment IV (spreadsheet *MCNP_BWR_Geometries.xls*, sheet *Thinning plates [Ni-Gd]*) based on the amounts of iron and aluminum contained within the basket cells. Iron was assumed to form the mineral Hematite (Fe_2O_3), and aluminum was assumed to form into the mineral Gibbsite ($Al[OH]_3$).

Current degradation rate information (Williams 2004) for the Ni-Gd alloy indicate that the maximum amount of degradation will be less than 1 mm per side, resulting in a minimum of 3 mm of Ni-Gd absorber remaining. Since geochemistry calculations for this material and waste package configuration are not available, varied amounts of estimated corrosion product composition were evaluated. The corrosion products represented come from the fuel basket tubes and thermal shunts, with the amounts varied from 0% to 100%. The Ni-Gd absorber corrosion products were represented as being removed from the system since this would decrease the amount of neutron absorber present (therefore increasing system reactivity). The configurations were evaluated using the 7x7 assembly design with 5.0 wt% U-235 fresh fuel. The results for this set of cases are presented in Table 31.

Table 31. k_{eff} Results for 3mm Thick Absorber Plate Cases

Corrosion Product Retained	k_{eff}	σ	Filename
0%	0.94116	0.00056	u0cp
33%	0.93027	0.00053	u33cp
66%	0.92652	0.00053	u66cp
100%	0.92770	0.00049	u100cp

These results indicate that the configuration is more reactive without corrosion product composition represented in the basket cells.

Table 32 illustrates results as a function of absorber plate (Ni-Gd Alloy) thickness, with 100% corrosion product retention.

Table 32. k_{eff} Results as a function of Absorber Plate Thickness

% Absorber Plate Removed	Remaining Plate Thickness (mm)	k_{eff}	σ	Filename
0	5	0.92662	0.00051	d0u
10	4.5	0.92724	0.00052	d10u
20	4.0	0.92713	0.00054	d20u
30	3.5	0.92742	0.00056	d30u
40	3.0	0.92770	0.00049	d40u

Results indicate that with 100% corrosion product retention, results are within one sigma (within statistical uncertainty of calculation) for 0 to 20% plate removal, and within two sigma through 40% plate removal. Therefore, the plates have the same relative effectiveness at 5 mm and 3 mm thickness.

I.8 COMPROMISED FUEL RODS

This configuration class is based on the waste form degrading before or at the same rate as the waste package internal structures and is representative of configuration classes IP-1 and IP-2 from YMP (2003, Figure 3-2). Seismic studies have determined that a peak ground velocity of 1.067 m/s or greater results in fuel cladding failure (BSC 2004g, Table 30) which results in exposure of the spent nuclear fuel to an oxidizing atmosphere. Once the fuel cladding is breached, oxidation of the fuel material can occur and cause clad breach propagation (unzipping). Therefore, a set of cases was evaluated that involved oxidized fuel. The thermodynamically stable state for oxidized uranium is UO_3 (Einziger 1991, p. 88). If moisture is present in the atmosphere hydration may also occur (Einziger 1991, p. 88) and form the compound $UO_3(H_2O)_2$ (Einziger 1991, Figure 1) otherwise known as the mineral schoepite (BSC 2004f, Attachment I, file *data0 files.zip*, file *data0.ymf*).

A set of sensitivity studies was performed in order to evaluate various configurations. The cases used a 5.0 wt% U-235 fresh fuel schoepite composition for each of the runs. The compositions were derived in Attachment IV (spreadsheet *schoepite.xls*, sheet *scoping*) for the fuel material in conjunction with spreadsheet *MCNP_BWR_Geometries.xls*, sheet *Sch kinf*. Mineral densities used

in the spreadsheets were taken from Roberts (et. al 1990). The results and a brief description of the cases are provided in Table 33.

Table 33. Compromised Fuel Assembly Sensitivity Cases

Filename	Case Description	k_{∞}	σ
Case0	Fresh fuel base case for comparison	1.01259	0.00129
Case1	Schoepite expanded around clad; nominal standard vertical geometry; dry conditions	1.07354	0.00107
Case2	Schoepite expanded around clad; aluminum shunts and fuel basket tube have corroded into gibbsite ^a and goethite ^b , respectively, occupying original volumes; nominal standard vertical geometry, dry conditions	1.00583	0.00119
Case3	Same as Case2 but the gibbsite and goethite volume expansion is represented along active fuel length	0.9781	0.00119
Case4	Same as Case1 but the system is compressed to the point where the basket plates are in contact with the fuel basket tubes	1.07381	0.00102
Case5	Same configuration as Case4 but the basket plate materials and fuel basket tube have oxidized into gibbsite and goethite	1.01587	0.0012
Case6	Same as Case5 but the waste package compression is in the vertical direction with expansion in the x direction	1.015	0.00117
Case7	Like Case2 but fuel basket tube is represented as hematite ^c instead of goethite	1.03268	0.00117
Case8	Same as Case5 but the fuel basket tube is hematite instead of goethite	1.03903	0.00118
Case9	Same conditions as Case1 but system is fully collapsed so there is no spacing between channel, fuel basket tube, and basket	1.08936	0.00107
Case10	Same as Case3 but the fuel basket tube corrosion product composition has settled within the basket cell and assembly is in standard horizontal position geometry (See Figure 7)	1.02600	0.00119
Case11	Same as Case1 but water fills all void space	0.98175	0.00115

NOTES: ^a Typical mineral oxidized aluminum forms into (Al[OH]₃)

^b Typical mineral iron forms into (FeOOH)

^c Typical mineral iron forms into (Fe₂O₃)

I.9 WASTE PACKAGE INTERACTION

A set of cases was evaluated to assess the impact of package-to-package interaction during preclosure operations. Variations were made in the spacing and interstitial material between packages to observe the sensitivity to such parameters. The interstitial material was represented as void and water, and the spacing was varied from 0 to 1 cm. A brief description of each case and the results are presented in Table 34.

Table 34. Waste Package Interaction Results

Case Description	k_{eff}	σ	Filename
Single waste package with no others, filled with water and void outside	0.96688	0.00054	7x7vr
Infinite array of waste packages touching, water inside and void outside	0.96507	0.00052	c1
Infinite array of waste packages touching, void inside and water outside	0.38419	0.00021	c2
Infinite array of waste packages touching, water inside and water outside	0.96592	0.00056	c3
Infinite array of waste packages with 1 cm spacing, water inside and void outside	0.96656	0.00058	c4
Infinite array of waste packages with 1 cm spacing, void inside and water outside	0.38018	0.00024	c5
Infinite array of waste packages with 1 cm spacing, water inside and water outside	0.96673	0.00056	c6

These results indicate that waste packages have a negligible neutronic influence on other waste packages.

INTENTIONALLY LEFT BLANK

Attachment II: Alternative Neutron Absorber Evaluation

Since the loss of neutron absorber precludes the ability to load the 44-BWR waste package, alternative means for criticality control were evaluated. These cases were just a set of scoping studies performed in order to evaluate the effects of alternative materials on a representative waste package configuration. Candidate materials were evaluated in order to determine the relative impact on criticality control for the waste package. The materials were selected based on the assumption that their corrosion resistance is adequate for 10,000 years. Due to their superior corrosion resistance, it is assumed that the absorber basket maintains structural integrity in these evaluations.

The candidate materials selected and evaluated are as follows:

- Ni-Gd Alloy - Gd loadings of 2.1, 1.9, 1.5, 1.0, and 0.5 wt%
- Alloy 22 (SB-575 N06022) with compartmentalized absorber blocks - ZrB_2 and B_4C were evaluated, both at the following B^{10} loadings: 18.4, 50.0, 99.0 wt%

An intact basket configuration corresponding to that used for the preclosure configuration was evaluated to determine the effects on system reactivity of changing the material composition of the absorber material. The base geometric configuration is illustrated below in Figure 10. For the compartmentalized absorber cases, the geometric arrangement is illustrated in Figures 11 and 12.

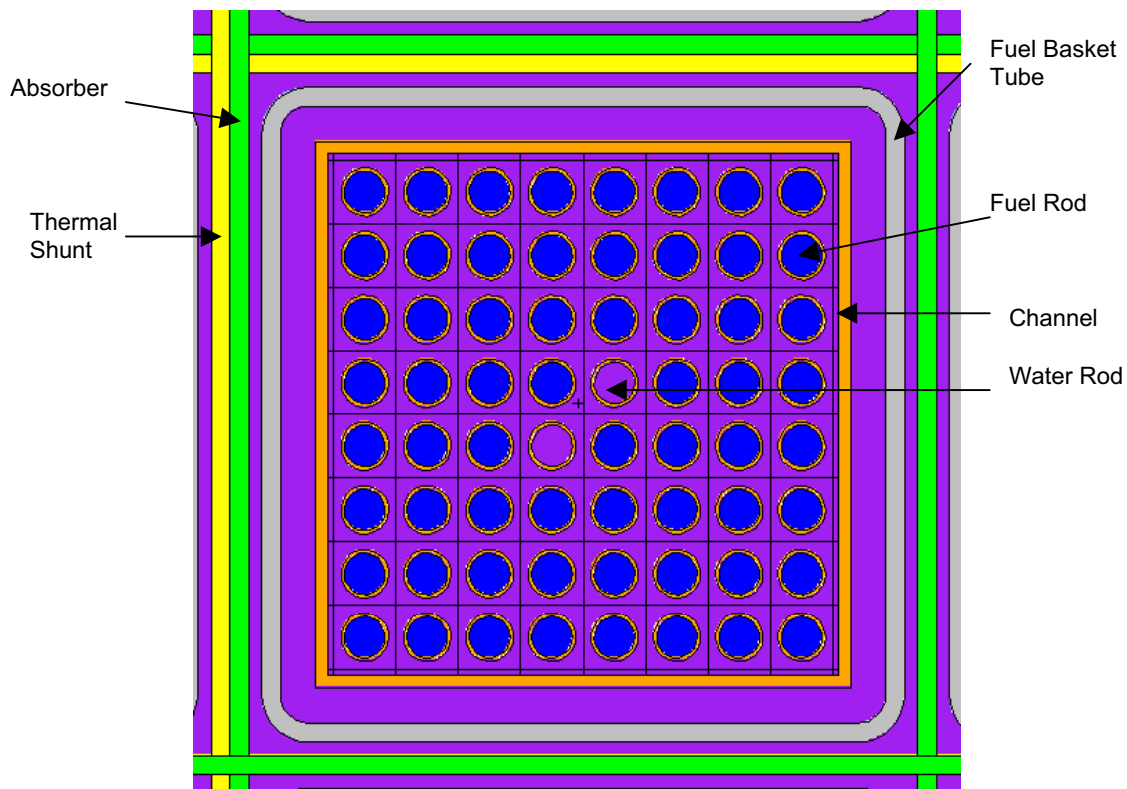


Figure 10. Base Geometric Arrangement

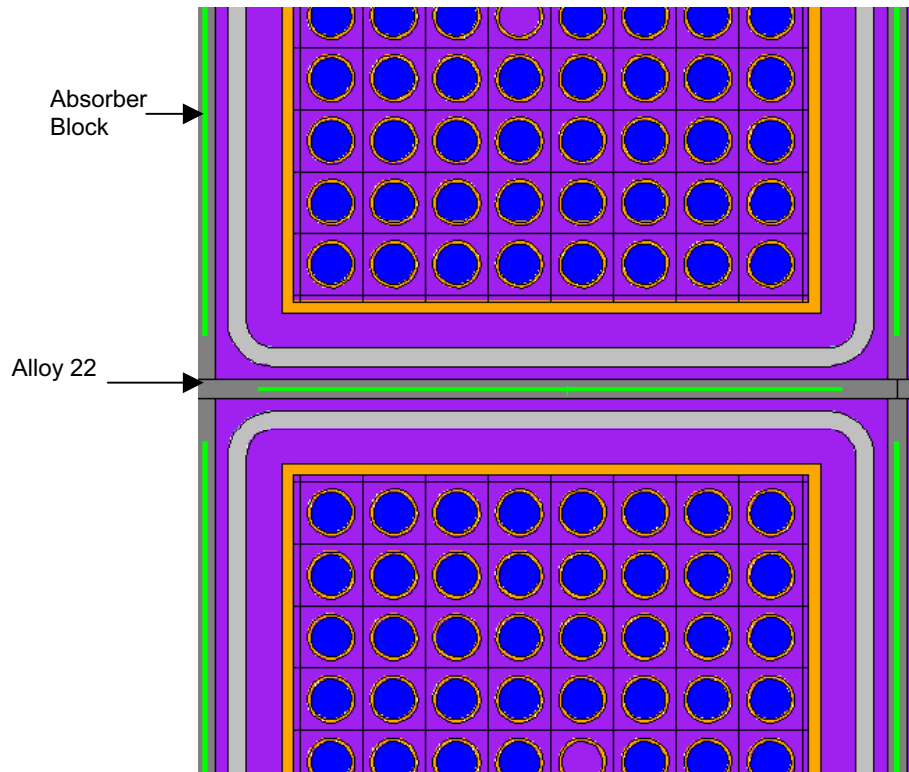


Figure 11. Top View of Absorber Blocks Encased in Alloy 22

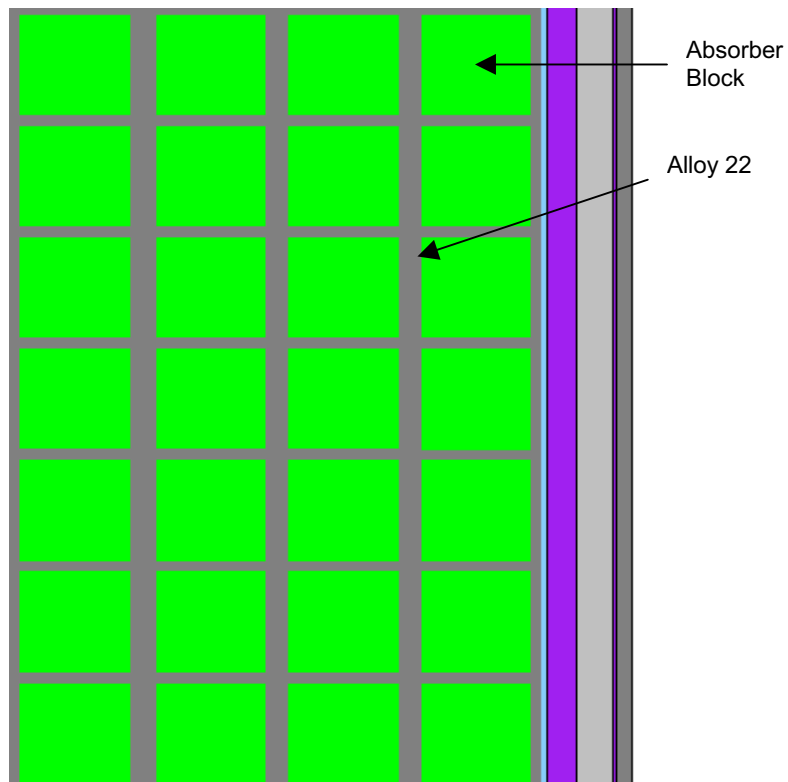


Figure 12. Side View of Absorber Blocks Encased in Alloy 22

The derivation of the parameters for the input files was made in Attachment IV (spreadsheet *MCNP_BWR_Geometries.xls*, sheets *plug geo* and *special mats*). In these specifications, the absorber material compositions were represented at 75% of the theoretical density values from Lide (2002, pp. 4-47 and 4-96). The 75% value is typically the maximum amount of credit granted by the NRC for fixed neutron absorbers (NRC 2000, p. 8-4).

Table 35 provides a listing of the results of the sensitivity studies in terms of their relationship to the base preclosure case (taken from Section 6). Each case evaluated used 5.0 wt% U-235 fresh fuel in a 44-BWR waste package configuration.

Table 35. BWR Waste Package Configuration Neutron Absorber Sensitivity Results

Material Description	k_{eff}	σ	Δk_{eff}^a	Equivalent Enrichment offset from LC
Ni-Gd alloy with 2.1 wt% Gd	0.97027	0.00054	0.0050	-0.099
Ni-Gd alloy with 1.9 wt% Gd	0.97218	0.00050	0.0030	-0.059
Ni-Gd alloy with 1.5 wt% Gd	0.97522	0.00052	0.0000	0.000
Ni-Gd alloy with 1.0 wt% Gd	0.97984	0.00059	-0.0046	0.086
Ni-Gd alloy with 0.5 wt% Gd	0.98845	0.00055	-0.0132	0.246
Compartmentalized Alloy-22 with B ₄ C (nat B)	0.91234	0.00057	0.0629	-1.449
Compartmentalized Alloy-22 with B ₄ C (50 wt% B10)	0.87434	0.00053	0.1009	-2.384
Compartmentalized Alloy-22 with B ₄ C (99 wt% B10)	0.84716	0.00053	0.1281	-3.053
Compartmentalized Alloy-22 with ZrB ₂ (nat B)	0.92895	0.00058	0.0463	-1.040
Compartmentalized Alloy-22 with ZrB ₂ (50 wt% B10)	0.89308	0.00058	0.0821	-1.923
Compartmentalized Alloy-22 with ZrB ₂ (99 wt% B10)	0.86659	0.00058	0.1086	-2.575

NOTE: ^a Δk_{eff} = loading curve material case k_{eff} minus new material k_{eff}

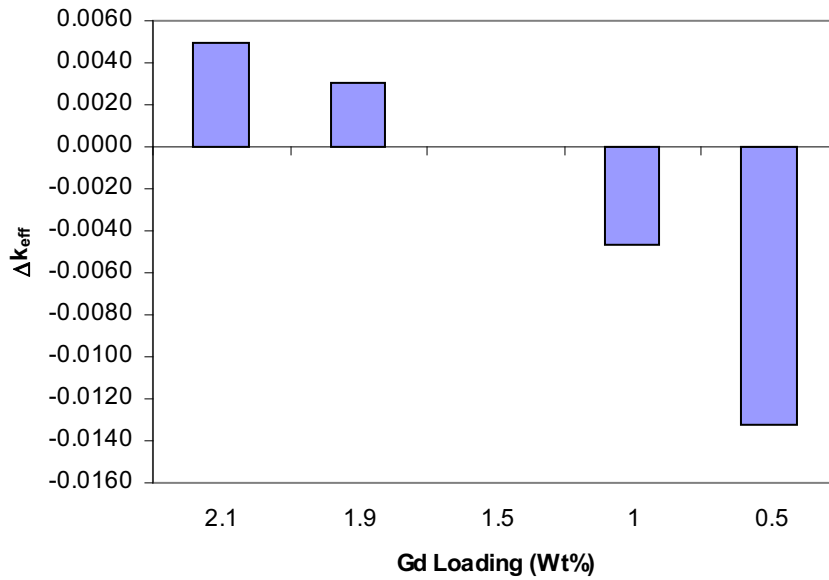


Figure 13. Effects on k_{eff} as a function of Gd loading

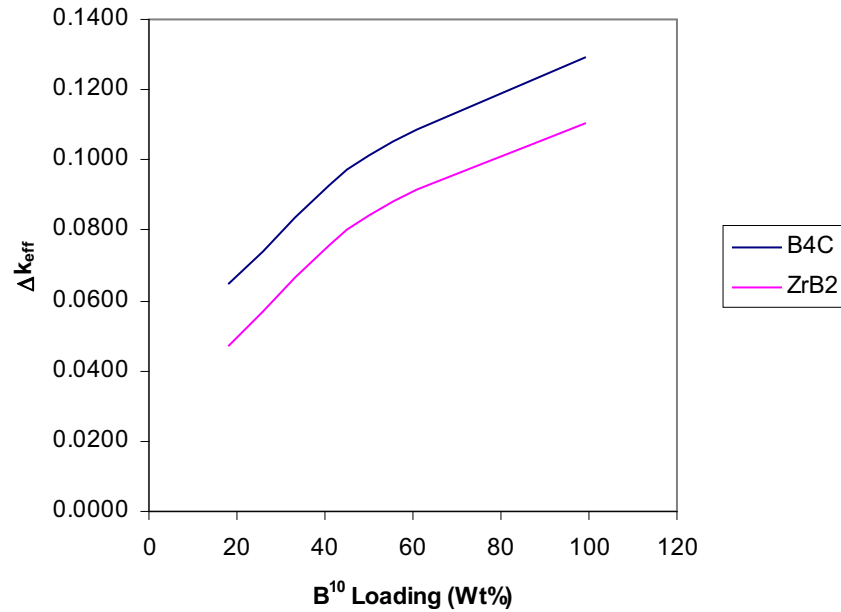


Figure 14. Effects on k_{eff} as a Function of B^{10} Loading

Below shows the relative impact on the 44-BWR waste package loading curve taken from Section 6 from using the alternative neutron absorber materials. These results are only intended to illustrate the relative effects of the different absorber materials. The results are based on taking Δk_{eff} using the alternative material in the preclosure configuration with a 5.0 wt% U-235 fresh fuel enrichment against the 1.5 wt% Gd, Ni-Gd Alloy with 5.0 wt% U-235 fresh fuel case used in Section 6.1.

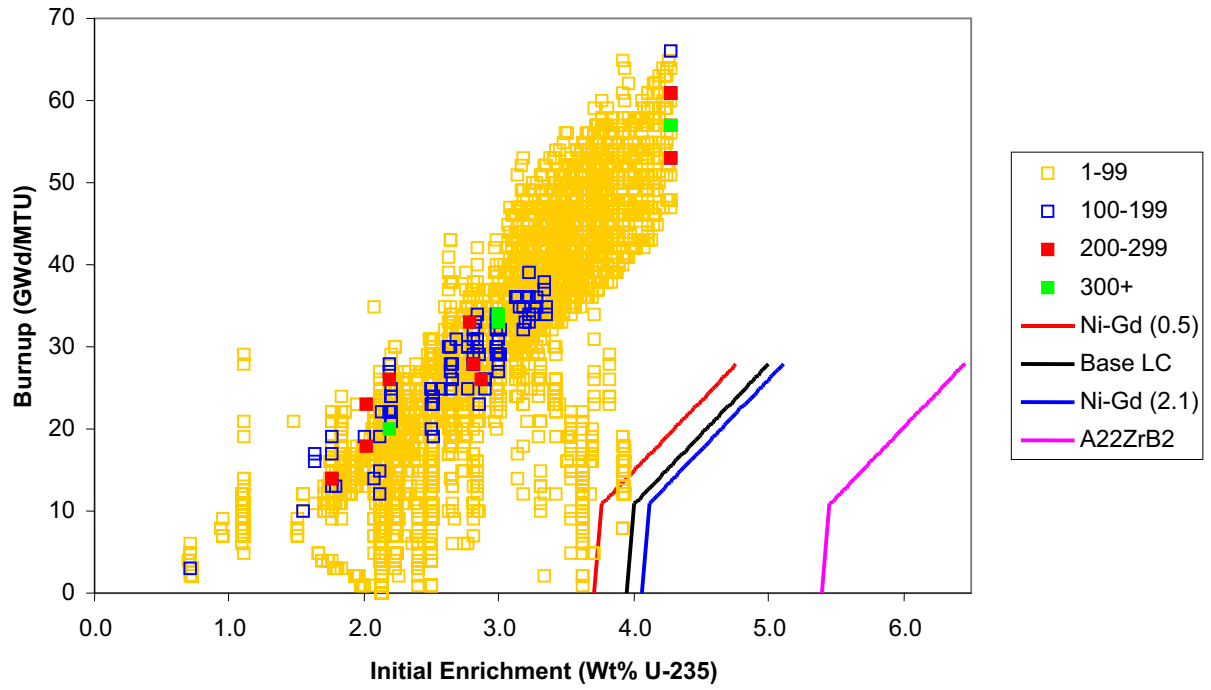


Figure 15. Loading Curve and Waste Stream Comparison

INTENTIONALLY LEFT BLANK

Attachment III: Attachment CD Listing

This attachment contains a listing and description of the files contained on the attachment CD of this report (Attachment IV). The CD was written using ROXIO Easy CD Creator 5 Basic installed on CRWMS M&O tag number 150527 central processing unit, and can be viewed on most standard CD-ROM drives. The zip archive was created using WINZIP 8.1. The file attributes on the CD are as follows:

<u>Filename</u>	<u>File Size (bytes)</u>	<u>File Date</u>	<u>File Time</u>	<u>Description</u>
44BWRWP.zip	1,465,133	8/19/2004	05:03p	44-BWR Waste Package Configuration Design Drawings
0130223.pdf	68,126	6/10/2004	10:03a	MSDS for representative hydraulic fluid
cases.zip	12,241,204	8/19/2004	04:31p	Archive containing MCNP files
GEassembly_Vol.xls	39,936	7/29/2004	10:44a	Excel spreadsheet containing tie plate material derivations
MCNP_BWR_Geometries.xls	797,696	8/13/2004	10:31a	Excel spreadsheet containing various geometry derivations
schoepite.xls	48,128	8/18/2004	01:36p	Excel spreadsheet containing schoepite material derivations
Tuff composition.xls	49,152	8/10/2004	10:53a	Excel spreadsheet containing tuff composition derivations
wstreamplot.xls	295,936	8/04/2004	03:45p	Excel spreadsheet containing sorted waste stream information

There are 8 total files for the archive file *44BWRWP.zip* with no particular naming system. The files contain the dimensions for the 44-BWR waste package configuration.

There are 276 total files (not including folders) contained in a unique directory structure for the archive file *cases.zip*. Files without an "o" at the end are input files, and files with an "o" at the end are output files. The following extracted directory structure corresponds as follows:

/Documents and Settings/scaglionej/My Documents/temp/:*

where * corresponds as follows:

- /I.1/* - Contains files listed in Attachment I, Section I.1
- /I.2/* - Contains files listed in Attachment I, Section I.2 with subdirectories *smear* and *unsmear* corresponding to smeared and unsmear pellet density cases, respectively.
- /I.3/* - Contains files listed in Attachment I, Section I.3
- /I.4/* - Contains files listed in Attachment I, Section I.4 with subdirectories *Hyd_Fluid* and *Water_density* corresponding to hydraulic fluid and water density cases, respectively.
- /I.5/* - Contains files listed in Attachment I, Section I.5
- /I.6/* - Contains files listed in Attachment I, Section I.6 with subdirectories *Tuff External*, *Tuff Internal Config 1*, and *Tuff Internal Config 2* corresponding to the tabulated results in Attachment I, Tables 28, 29, and 30, respectively.
- /I.7/* - Contains files listed in Attachment I, Section I.7 with subdirectories *3mm* and *Thickness* corresponding to the tabulated results in Attachment I, Tables 31 and 32, respectively.

/I.8/ - Contains files listed in Attachment I, Section I.8

/I.9/ - Contains files listed in Attachment I, Section I.9

/Pre_LC/ - Contains files used for the preclosure loading curve configuration as a function of burnup where the naming system is as follows: *XXYY* where the *XX* represents the initial enrichment in wt% U-235 (i.e., 35 is 3.5 wt% U-235 [range from 3.5 to 5.0 wt% U-235]) and the *YY* represents the burnup in GWd/MTU (range from 10 to 40 GWd/MTU). A lower level directory denoted */Fresh/* contains the fresh fuel cases with a naming system as follows: *X.X* that represents the enrichment in wt% U-235 (ranging from 3.0 to 5.0).

/Post_LC/ - Contains files used for the postclosure loading curve configuration as a function of burnup where the naming system is as follows: *XXYY* where the *XX* represents the initial enrichment in wt% U-235 (i.e., 35 is 3.5 wt% U-235 [range from 4.0 to 5.0 wt% U-235]) and the *YY* represents the burnup in GWd/MTU (range from 10 to 20 GWd/MTU). A lower level directory denoted */Fresh/* contains the fresh fuel cases with a naming system as follows: *X.X* that represents the enrichment in wt% U-235 (ranging from 3.0 to 5.0).

/II/ - Contains the files from Attachment II with a naming system as follows: *aXp7YYY* where the *X* is either a 2 or a 3 denoting B₄C or ZrB₂ as the absorber, respectively; and the *YYY* is either n, e50, or e99 denoting the B¹⁰ loading as nominal, 50 wt%, or 99 wt%, respectively. Within this directory is a lower level directory denoted */Gd Enr/* which contains the files where the Gd loading in the Ni-Gd Alloy was varied. The naming system corresponds as follows: *X.X* which represents the Gd loading weight percent (i.e., 0.5 = 0.5 wt% Gd).